Constraining Mesozoic early post-rift depositional systems evolution along the eastern Central Atlantic margin

Angel Arantegui[a,*] Rhodri Jerrett[a] Stefan Schröder[a] Luc G. Bulot[a,b] Roberto Gatto[c] Stefano Monari[c] Jonathan Redfern[a]

[a]School of Earth and Environmental Sciences, University of Manchester, M13 9PL, Manchester, United Kingdom

[b]Aix-Marseille Université, CNRS, IRD, Coll France, CEREGE, France

[c]Dipartimento di Geoscienze, Università di Padova, Italy

*Corresponding author. E-mail address: angelarantegui@hotmail.com

Abstract

Extensive Mesozoic outcrops exposed in the Aaiun-Tarfaya Basin, in the Atlantic margin of Morocco, have been overlooked for decades. Original subdivisions and dating of rocks, performed more than five decades ago, have survived until today virtually without any update. In the north eastern margin of the basin, key Mesozoic sections have been revisited. Its coastal position next to the Variscan Anti-Atlas Orogen allows insight into the interplay between local tectonics and eustasy during deposition of sedimentary sequences on passive margins. High-resolution stratigraphy and sedimentology have allowed for an improved understanding of the depositional systems and evolution during the early opening of the Atlantic and provided a valuable control point recording the syn- and early post-rift evolution of the basin. Three formations are described: (i) a basal continental red bed unit unconformably overlying the Palaezoic Variscan basement of the Ifni Inlier; (ii) a unit dominated by intertidal clastics and microbial carbonates, and (iii) a shallow marine unit comprising mixed siliciclastic-carbonates. Despite the sedimentological affinity of these outcrops to Triassic or Lower Jurassic deposits elsewhere in Morocco, these units had previously been assigned an Early Cretaceous age, based on limited non-conclusive fossil fauna and basin-scale lithostratigraphic correlation. New collections of macrofauna have yielded a Bathonian age for the upper part of the succession and a possible Triassic/Early Jurassic for the lower part. The whole succession displays an overall transgressive trend not consistent with the eustatic Bathonian sea-level fall. Local post-rift tectonic pulses exhuming the Western Anti-Atlas coupled with eustasy are responsible for increased sediment supply at this time. Enhanced tectonic subsidence, overcoming sea-level fall, is interpreted to be the main driver for creation of accommodation and preservation of this sequence. Resumed sedimentation on structural heights offshore suggests exhumation of the Western Anti-Atlas ceased by the early Callovian, reducing clastic input to the region and allowing the development of a carbonate platform. Variable regional exhumation and local tectonics along the Moroccan margin during the early post-rift stage

influenced the highly variable nature of clastic vs carbonate deposition, thickness distribution and depositional environments at this time.

Keywords: Basin Analysis; Northwest Africa; Morocco; Aaiun-Tarfaya Basin; Biostratigraphy; Bathonian

1. Introduction

The Atlantic margin of Morocco has been undergoing an increase in hydrocarbon exploration activity in the last decades, but still remains relatively underexplored. Thick Mesozoic offshore successions have been drilled along the margin, targeting both clastic and carbonate reservoirs. The results to date, with sparse hydrocarbon shows and some uncommercial discoveries point to working petroleum systems, but a better understanding of the stratigraphy, sedimentology and overall evolution of the Moroccan passive margin is needed.

In the Aaiun-Tarfaya Basin (Fig. 1), scattered oil shows and three uncommercial discoveries suggest hydrocarbon potential, but successive wells drilled offshore keep missing the main reservoir. This low rate of success points to a limited comprehension of the evolution of depositional systems through time and highlights the need of updated stratigraphic and sedimentological studies. Since the pioneering outcrop-based studies in the 1940's to 1960's on the regional geology (Alía Medina, 1945, 1952; Choubert and Marçais, 1956; Martinis and Visintin, 1966; Querol, 1966) and definition of the main sedimentary units in the basin, there has been little to no update on the Mesozoic geology. The understanding of the Mesozoic sedimentary fill of the Aaiun-Tarfaya Basin has been moved forward only from subsurface studies (e.g., El Khatib et al., 1995, 1996; Le Roy et al., 1997; Abou Ali et al., 2005; Elbatal et al., 2010; El Jorfi et al., 2015), while the outstanding onshore Mesozoic exposures present in the basin have been overlooked.

[Insert fig. 1 here]

Within the Mesozoic of the northern half of the Aaiun-Tarfaya Basin (see Tarfaya and Ifni segments in Fig. 2) only three formations have been described (Martinis and Visintin, 1966). The Upper Jurassic marine carbonates of the Puerto Cansado Formation are not exposed in the basin and are known only from exploration wells. The Cretaceous is extensively exposed onshore and was subdivided in two formations. The basal, mainly continental Tantan Sands Formation are of Early Cretaceous age and the marine Aguidir Limestones Formation are of Albian to Maastrichtian age. Biostratigraphic control of these units is relatively poor and based on old datasets (Choubert et al., 1966; Collignon, 1966; Martinis and Visintin, 1966; Viotti, 1965, 1966). Notably, in recent publications (Benziane et al., 2016), detritic red facies from the Early Cretaceous and undifferentiated “middle” Cretaceous units are still reported, with dating of successions based on arguably identified fossil groups.

[Insert fig. 2 here]

This study examines the Mesozoic coastal section exposed along the Atlantic flank of the Ifni Inlier (Fig. 4), traditionally reported as Early to "middle" Cretaceous in age. The sedimentary succession provides a record of the early syn-rift stage of the passive margin as the Atlantic opened. Extensive fieldwork has been undertaken, with detailed logging together with sampling for new biostratigraphic dating, in order to investigate the controls of sedimentation, depositional and tectonic history of the basin. A new Bathonian (Middle Jurassic) age, together with detailed sedimentological logging has allowed the establishment of a new stratigraphy and depositional model, a better understanding of the interplay between tectonics and eustasy in this part of the basin and a comparison of the Jurassic stratigraphy along the Moroccan Atlantic basins.

2. Geological setting

The Mesozoic basins along the Atlantic margin of Morocco (Fig. 1) developed in response to rifting and subsequent breakup of Pangaea. Rifting along the Central Atlantic segment, between northwest Africa and North America started in the Late Triassic, generating grabens and half-grabens oriented approximately NE-SW (Bouatmani et al., 2004). Restricted basins were initially filled with coarse alluvial and fluvial syn-rift clastics and evaporites (van Houten, 1977; Brown, 1980; Abou Ali et al., 2004, 2005). From the very latest Triassic/beginning of the Jurassic (c. 201-–190 Ma), extensive tholeiitic magmatic activity (Fig. 1) occurred within the Central Atlantic Magmatic Province (CAMP; e.g., Wilson and Guiraud, 1998; Davies et al., 2017). The timing of onset of the drift phase and creation of the first oceanic crust on the African side is postulated between the Early and Middle Jurassic (e.g., Klitgord and Schouten, 1986; Scotese, 1991; Steiner et al., 1998; Sahabi et al., 2004; Schettino and Turco, 2009; Labails et al., 2010; Biari et al., 2017). During late Early Jurassic open marine conditions were established along the margin of NW Africa (Jansa and Wiedmann, 1982). Carbonate platforms were widespread from the Middle to Late Jurassic, forming a more-or-less continuous carbonate shelf <2 km thick and extending along the northwest African margin (Jansa and Wiedmann, 1982). In the deep basins, time equivalent marls, fine clastic- and calci-turbidites were deposited (Fig. 2). Carbonate production continued until the Early Cretaceous, when increased terrigenous delivery to the basins and establishment of a number of deltas along the margin, such as the Tantan and Boujdour systems in the Aaiun-Tarfaya Basin (Martinis and Visintin, 1966; Einsele and von Rad, 1979; Davison, 2005) eventually shut off carbonate production.

The Aaiun-Tarfaya Basin trends NE-SW (Fig. 1) and extends along the Moroccan Atlantic margin for c. 1100 km, with an approximate onshore area of 170,000 km^2. It is bounded by the western termination of the Pan-African and Variscan Anti-Atlas mountain belt to the northeast; the Palaeozoic Tindouf/Zag Basin to the east; and the Reguibat Shield and Mauritanides (Adrar Soutouf and Zemmour) to the southeast (Fig. 1). Upper Triassic (Norian) syn-rift clastics were deposited together with thick evaporite sequences offshore (Fig. 2). Open marine conditions were only established in the Sinemurian, followed by a Pliensbachian to

Callovian carbonate platform. Later regressive marine sandstones were deposited, capped by a renewed transgression leading to deposition of open marine carbonates (du Dresnay, 1988; Zühlke et al., 2004; Abou Ali et al., 2005; Davison, 2005). Onshore and offshore, well and seismic data (Viotti, 1966; Abou Ali et al., 2005; Michard et al., 2008b) indicates the Late Jurassic is represented by an extensive carbonate platform, the Puerto Cansado Formation. (Martinis and Visintin, 1966) with reefal build-ups along the platform margin. Salt remobilisation started in the Early Cretaceous representing the dominant structural driving force in this period (Zühlke et al., 2004; Michard et al., 2008b). The platform margin slope collapsed during the Berriasian eustatic lowstand, and some of the Jurassic succession was eroded.

3. Methods

The studied succession is exposed inland along outcrops cut by the Oued (Arabic for ephemeral river) Craima and along coastal sections from Legzira (Guezira) Beach to Foum Assaka (Fig. 4). The most continuous exposures are located along Oued Craima and Sidi Ouarzik Beach. The resulting sedimentary log is over 550 m thick and was logged at a cm scale, identifying lithological changes, sedimentary structures, trace and body fossil content, in order to undertake facies analysis. A total of 53 samples, representative of different sedimentary facies, were collected and thin-sectioned for microfacies and petrographic characterisation. The thin sections were stained with alizarin red-S and potassium ferricyanide (Dickson, 1966) to enhance different types of shells and generations of carbonate cements; and with potassium rhodizonate for plagioclase and K-feldspar identification (Bailey and Stevens, 1960). Additionally, 20 fossiliferous levels were sampled for macrofauna analysis in order to aid in environmental interpretations and refine dating of the succession. Samples were prepared with standard mechanical and chemical methods for extraction/cleaning of mollusc specimens at the University of Padova (Italy). About 300 gastropods and bivalves were studied in detail and identified to species level whenever possible. Specimens were photographed using the focus stacking method and the digital images processed with Helicon Focus Pro 6.7.1 software. All levels sampled are indicated on the sedimentary log.

4. Facies analysis

A composite sedimentary log of the studied succession along Oued Craima and Sidi Ouarzik Beach is shown in Fig. 5. The position of the samples collected for thin-section analysis and macrofauna are shown on the log. Twenty five lithofacies have been defined (see Supplementary material for detailed description of each lithofacies) and grouped into seven Facies Associations (FA).

4.1. FA 1 (Alluvial Fan)

This association is entirely made of red-coloured conglomerates, subordinated sandstones and silts lacking any kind of fossil content (Fig. 6). It is composed predominantly of normally graded to massive clast-

supported conglomerates with boulders up to 60 cm in diameter (lithofacies A) without sedimentary structures. Individual beds are up to 1 m thick, have undulating, sharp and erosive bases. Beds usually are laterally continuous at outcrop scale or pinch out, rarely channelized with a maximum lateral extension of 20 m. Occasional inversely graded conglomerates (lithofacies B) up to 50 cm thick are present. They are usually discontinuous and with smaller grain size. Cross-bedded sandstones range in grain size from fine to very coarse, with lags of granules and pebbles (lithofacies D). Very fine- to fine-grained massive sandstones (lithofacies G) are up to 50 cm thick. There is a total lack of biogenic structures in this facies association and sedimentary structures are extremely rare along Oued Craima.

Interpretation: The clast size and presence of erosive sharp bases suggest high-energy flows. The absence of sedimentary structures and sheet-like nature of beds is indicative of ephemeral unconfined flows related to flash floods events in an alluvial fan environment. Intervals which lack interbedded sandstones represent a proximal setting, where avulsion and switching of active lobes is common. The alternation of sandstones and conglomerates is interpreted to record a variation in flow regime, possibly indicating the lateral switching of lobes on the fan in a more medial location. The absence of palaeosols or rootlets in the finer sediments suggests high rates of sedimentation, erosion and short exposure time between flows.

4.2. FA 2 (Alluvial floodplain)

This association is composed of c. 50 cm thick beds of white fine-grained rippled-cross laminated sandstones fining into very fine-grained red silty sandstones displaying pedogenetic mottling and rootlet traces (lithofacies H), interbedded with discrete conglomerate beds (lithofacies A and B) up to 40 cm thick (Fig. 6). The rippled white sandstones typically have sharp, non-erosive basal contacts with the red sandstones. Clasts include quartz, detrital dolomite and feldspars, cemented by calcite and iron-rich patches. The interbedded conglomerates have sharp erosive bases, lack sedimentary structures and the clast size is up to 25 cm in diameter.

Interpretation: Rippled white very fine-grained sandstones grading into red silty sandstones with discontinuous lamination are indicative of lower regime unidirectional flows in unconfined conditions. Periods of low sedimentation rates and plant colonisationcolonization are suggested by presence of pedogenetic features in these finer grained sediments (Fig. 6; A, B). Interbedded conglomerates are interpreted as high-energy deposits of unconfined flows, possibly debris flows.

4.3 FA 3 (Peritidal coastal plain)

Peritidal deposition occurs in a wider zone than the intertidal zone, and includes the shallow subtidal and supratidal environments (e.g., Wright, 1984; Spence and Tucker, 2007; Allaby and Argyll, 2008). This association is represented by fining upwards mixed clastic-carbonate packages between 3 and 10 m thick (Fig. 7). An ideal succession of this association includes a carbonate-dominated base and clastic-dominated

middle and upper part. The basal part of these packages is usually made of oncoidal packstones, peloidal-bioclastic and bioclastic-oolitic grainstones (lithofacies P, V and O). Oncoidal packstones (lithofacies P) is the most abundant lithofacies at the base of the fining-upward packages, composed mainly of mm-scale porostromate oncoids, peloids, carbonaceous plant fragments, ostracods, microbial/algal lumps and intraclasts. Cross-bedded bioclast-ooid-bearing grainstones (lithofacies O) commonly show erosive and channelized bases up to 1.2 m deep cutting into grainstones of lithofacies V. The former include terrestrially-derived igneous and metamorphic rock fragments, algal/bacterial mat fragments, and broken echinoderm and mollusc bioclasts, all of which can constitute the nucleus of ooids up to 2.5 mm in diameter. The latter appears in massive to laminated beds up to 30 cm thick mainly made up of molluscs, peloids and benthic foraminifera (agglutinated, miliolids and textulariids). Subordinate components include carbonaceous plant fragments, ooids and dasyclads. Calcareous siltstone-sandstone, micritic mudstone and matrix-supported conglomerate (lithofacies Q, R and C) locally occur in the basal part of packages. Carbonate-rich lithofacies Q and R are frequently massive with sharp undulating bases and occasionally affected by soft sediment deformation. Main grains include bioclasts (molluscs, ostracods, foraminifera and algae), carbonaceous plant fragments and quartz clasts. Bioturbation can be intense in individual beds. The middle parts of the fining upwards packages are dominated by siltstones to very fine-grained rippled sandstones (lithofacies L), punctuated by cm-thick algal-laminated packstone interbeds (lithofacies N), which exceptionally can stack up to 1.2 m thick packages. Carbonaceous plant fragments are the main component in lithofacies L, which appears mostly fossil-free. Lithofacies N is made of interlaminated peloidal boundstones, microbial/algal stromatolite-like mats and peloidal packstones to wackestones composed mainly of clots of biologically-trapped silt-sized subspherical peloids and scattered fragments of reworked microbial/algal mats up to 2.5 mm in size. At the microscopic scale, it shows cyclic micrite- and siliciclastic-rich lamina, desiccation cracks and small amounts of marine bioclasts. This facies association is capped by carbonate-prone palaeosols (lithofacies J), sometimes alternating with siltstones and sandstones of lithofacies L.

Interpretation: Basal facies (lithofacies P, V) contain abundant marine fauna (milliolids, agglutinated foraminifera, ostracods, dasyclads) that lived in partly stressed shallow marine environments. Micritization is characteristic of early marine diagenesis. Oncoids in lithofacies P are typical of shallow subtidal to lower intertidal inner lagoons and shoals (Flügel, 2010) where a certain degree of agitation allows microorganisms to develop a cortex around a nucleus and can mark the beginning of transgressive sequences (Wright, 1983). Channelised cross-bedded grainstones (lithofacies O) and conglomerates (lithofacies C) reflect higher-energy depositional processes in this subtidal environment. The array of allochems with terrestrial and marine affinities, including plant fragments, and the characteristic channelised geometry suggest tidal channels and creeks.

The alternating fine sandstones and muds (lithofacies L) in the middle of fining-up packages are characteristic of mud and sand flats that are exposed to the constant action of tides. The associated minor siltstones-sandstones of lithofacies Q have erosive bases, reworked and broken bioclasts that indicate high energy and probably short-lived event beds. They are interpretated as storm- or high tide-related beds. Algal/bacterial-induced peloidal packstones and bindstones (lithofacies N) formed in intertidal algal marshes with initial carbonate soil development (Hardie, 1977). Desiccation cracks in this lithofacies record repeated periods of exposure and initial soil development (Ginsburg et al., 1977).
Under conditions of prolonged exposure, carbonate-rich palaeosols developed on fine-grained sandstones and muds (lithofacies J) and form the upper unit of the fining up packages.
The fining-upward profile and vertical succession of facies are interpreted as the progradation and shoaling of a tidal flat (e.g., Wright, 1984; Hardie, 1986; Flügel, 2010; Daidu et al., 2013). The basal carbonates and clastics (lithofacies P, V, O, C, Q and R) represent deposition in a shallow subtidal environment cut by tidal channels. They are overlain by intertidal clastics (lithofacies L) and algal carbonates (lithofacies N), and ultimately capped by supratidal palaeosols (lithofacies J). The inward part of the tidal flat would be exposed most of the time and only reached by storms and extreme tides (Ginsburg et al., 1977).

4.4 FA 4 (inner lagoon)

This facies association is exposed along Oued Craima and Sidi Ouarzik Beach. It comprises packages exhibiting a coarsening upwards profile composed of different lithologies ranging from barren fine-grained clastics to pure carbonates, usually fossil-rich (Fig. 8) and can be up to 6.5 m thick.
Most coarsening upwards packages start with laminated dark clays to very fine-grained sandstones (lithofacies M) grading into yellowish calcareous sandstones to packstones (lithofacies F) up to 2.7 m thick. The characteristic dark colour of these units is due to very abundant sub-mm-scale carbonaceous plant fragments delivered from a terrestrial source. These packages can be punctuated by cm to dm thick interbeds of bioclastic-peloidal and oncoidal wackestone/packstone (lithofacies S and P) and fine clastics with reworked carbonate clasts (lithofacies K). Occasionally, micritic mudstone (lithofacies R) can underlay the dark laminated fine clastics of lithofacies M. Main fossil groups found in FA4 include bivalves, gastropods, benthic foraminifera, green and red algae (Figs. 8, 10, 11). Many of the benthic foraminifera could be identified to genus level, and two of them to species level: *Nautiloculina oolithica* Mohler, 1938 and *Nautiloculina circularis* (Said and Barakat, 1958). Fish remains and echinoderm plates are minor components.
Interpretation: The absence of fauna typical of normal marine conditions, such as cephalopods and brachiopods, suggests a restricted environment with relatively stressed conditions, such as abnormal salinities in a lagoon or protected shelf (Aberhan et al., 2002). The identification of green algae (*Holosporella siamensis*, possibly *Marinella* sp. and unidentified dasyclads), possible cyanobacterial lumps

and benthic foraminifera (Nautiloculina spp.) also support a protected and shallow shelf/lagoon (Tasli, 2001). Sea urchins are very rare, but their regular tests also supports the interpretation of a protected, relatively low-energy environment. Abundant micrite envelopes on most types of grains is indicative of a shallow marine setting (Flügel, 2010).

The clastic intervals alternating with the silt-rich carbonate beds suggest an intermittent proximal source of clastics from the continent, interacting with the "carbonate factory" in the lagoon. The source of this clastic material may have been small-scale bayhead deltas prograding into the lagoon. Interlayered muds and very fine-grained sand (lithofacies M) with mm-scale erosive surfaces and the lack of burrowing and fauna is interpreted as the result of hyperpycnites (river-flood-generated turbidity currents) that would stress the environment, inhibiting colonization by organisms (Mulder et al., 2003).

[Insert fig. 3 here]

4.5 FA 5 (Outer lagoon)

FA5 is represented by limestone (lithofacies S, T and V; Fig. 8) packages up to 3 m thick, usually bounded by laminated fine-grained clastics (lithofacies M). Individual beds are 10–40 cm thick and tend to be massive, occasionally undulated and load-casted, wackestones, packstones and grainstones with peloids and bioclasts as main allochems. Bivalves and gastropods can reach several cm in size (see Figs. 10, 11). Additional groups that can be locally important are benthic foraminifera, echinoderms, ostracods and blue – green algae, together with carbonaceous plant fragments, quartz and feldspar clasts. Reworked carbonate clasts up to 7 cm may be present. Oolitic and algal grainstones (lithofacies W and U) are subordinate facies that appear as massive to irregularly bedded interbeds with a maximum thickness of 25 cm. Normal grading, cross-bedding, shell lags and mud drapes are possible but uncommon. Concentric micritic ooids, peloids and intraclasts (lithofacies W) and mm-scale blue–green algae fragments, together with intraclasts and terrigenous clastics (lithofacies U) are the main components. This facies association is occasionally punctuated by thin cm- to dm-thick beds of micrite (lithofacies R).

Interpretation: Common grainstone and packstone textures, absence of sedimentary structures, frequent load casts and less common interbedded fine-grained facies suggest periods of rapid deposition in a relatively energetic environment, punctuated by short-lived episodes of low energy conditions. The general paucity of green-blue algae and oncoids, together with a relative abundance of echinoderms and ooids over ostracods in some beds, suggest some connection with open marine conditions in more energetic waters. Reworked carbonate clasts also support the interpretation of an agitated environment under the influence of waves, tides and storms. Rare thin beds with highly irregular bedding, rich in green algae (lithofacies U) may be related with wash-over or back-shoal deposits reworking shallow marine fauna close to shoals.

4.6. FA 6 (Barrier-shoal complexes/Upper shoreface)

FA6 can be carbonate- or clastic-dominated. Where carbonate-dominated, FA6 is usually found underlying FA4 and interstratified with FA5. Where clastic-dominated, FA6 is usually found overlying FA7 and is more frequent in the upper 70 m of the succession exposed at Sidi Ouarzik Beach.

The carbonate-dominated FA6 is composed of massive peloidal/bioclastic and oolitic grainstones (lithofacies V and W) and cross-bedded oolitic grainstones (lithofacies X). Minor interbeds of bioclastic wackestones to packstones (lithofacies S) are recorded. Packages of FA6 are up to 4 m thick. They usually mark the base of fining upwards packages that evolve into FA4 (see P53 in Fig. 5). Palaeoflow orientations from foresets on cross-bedded grainstones after bedding restoration is directed towards 269° (n = 12) and foresets may be reworked by wave ripples.

The clastic-dominated FA6 is made of cross-bedded sandstones (lithofacies D), subordinate grainstones and packstones with peloids, and a wide range of bioclasts (lithofacies V and F) and sandstones with floating pebbles (lithofacies C). Bases are occasionally dewatered or load-casted and ripples may be present at the top of individual beds. Readings from the foresets of crossbedded sandstones yield palaeocurrents orientations directed towards 091° (n = 5). Minor intercalations of peloidal wackestones/packstones, ripple-laminated sandstones with climbing ripples and dark fine-grained clastics (lithofacies S, E and M) are also present.

Interpretation: Abundant grainstones and subordinate packstones together with frequent micritised grains in the carbonate-dominated lithofacies association suggest a high-energy environment and shallow water conditions. The dm-thick oolitic grainstones, that can be stacked in banks up to 3 m thick, are interpreted as oolitic shoals, also supporting an interpretation of shallow water conditions. Possible microkarst development on some beds (lithofacies W) supports periodic exposure of the shoals. Wave reworking on the cross-bedded grainstones (lithofacies X) represent subaqueous dunes formed under unidirectional currents in relatively shallow conditions above fair weather wave base. Palaeoflow directions towards the west are subparallel to the palaeocoast line suggesting the presence of longshore currents. The association of these sediments and interpreted processes suggests a high-energy very shallow barrier complex setting associated with a lagoon (FA 4 and 5).

The upper c. 70 m of the succession along Sidi Ouarzik Beach (Fig. 5) becomes increasingly siliciclastic. Lithofacies F and C are frequently massive and soft-sediment deformed sandstones record rapid sedimentation by unconfined flows due to sudden deceleration of the original flow. Wave ripples on the top surfaces of individual beds suggest reworking by waves and the presence of thin interbeds of muds represent suspension settling, possibly as a function of tidal influence, between higher discharge events. Due to the scale of these deposits (dm-scale to 1 m) they are interpreted as small-scale subaqueous bars. The presence of climbing ripples supports the notion of periodic events of higher discharge and high sediment supply. Wave ripples also suggest deposition above fair weather wave base. Unlike the carbonate-dominated FA6, here the absence of oolitic grainstones and association with FA7 (see below) is

interpreted as representing slightly deeper water conditions. The depositional setting is interpreted as upper shoreface (inner ramp) above fair weather wave base.

[Insert fig. 4 here]

4.7 FA 7 (lower shoreface/Middle ramp)

FA7 is represented by coarsening-upwards packages up to 2.5 m thick, which can stack to form successions up to 6.5 m thick. FA7 is mainly made of dark clays and fine-grained sandstones and cross-laminated sandstones with common hummocky cross-lamination (lithofacies M and I). Subordinate lithofacies include silty packstones and wackestones with peloids and bioclasts (lithofacies F and S), chaotic coral-bearing packstones with variable proportions of branching coral debris (lithofacies Y), and cm-thick micritic mudstones (lithofacies R).

Interpretation: The dark claystones represent suspension settling under low current velocities, whereas ripple cross lamination and hummocky cross stratified sandstones evidence episodic coarser sediment input and the occurrence of unidirectional and combined flows which may be storm induced. Overall, a lower shoreface setting, below fair weather wave base but above storm wave base, is likely for this association. The branching forms of coral were sourced from coral build-ups offshore, below fair weather wave base, that were reworked by storm waves.

5. Discussion

5.1. Depositional model

Seven FA have been described, grouped into three depositional environments representing continental (FA1 and FA2), peritidal (FA3) and marine (FA4-FA7) environments. The evolution of the Bathonian section shows an overall transgression, punctuated by continental clastics, conglomerate interbeds, interpreted to record pulses of uplift and erosion within the Western Anti-Atlas. After each tectonic pulse, the system stabilised and continuous basin subsidence resulted in transgression of peritidal to marine conditions, until the next tectonic pulse and renewed progradation.

Although deposited during the Bathonian global eustatic sea-level fall (Haq et al., 1987; Snedden and Liu, 2010), the succession records an overall transgressive pattern suggesting subsidence (thermal and/or tectonic) outpaced eustasy. Periods of coarse clastic progradation record the combined effect of local tectonic activity in the Anti-Atlas and the superposed sea-level fall.

The depositional model depicts four stages in the evolution of the coastal section at Oued Craima and Sidi Ouarzik Beach, on the flank of the Ifni Inlier (Fig. 9). The lower part of the succession (c. 180 m) comprises coarse alluvial fans deposited next to the prominent topography of the Ifni Inlier (Figs. 6, 9A). Intense subsidence in the basin extended to the coastal margin of the Ifni Inlier, that combined with progressive erosion and loss in topography to allow transgression and development of a thick peritidal succession (Fig.

5; from ~185–325 m). The significant amount of fine-grained clastics, together with carbonate-rich palaeosols, microbial mats and periodic marine-influenced beds, suggest the development of a fringing tidal flat attached to the Anti-Atlas (Fig. 9B). The tidal flat was wide enough to allow development of tidal creeks and marshes that supplied abundant carbonaceous plant material to the marine environment. A shallow lagoon is postulated along the shoreline, supplying oncoids, ostracods and other bioclasts inland, transported by tidal currents or storms. The upper c. 190 m of the succession is represented exclusively by marine sedimentation (Fig. 5) recording an overall water deepening; with lagoonal muds and bioclastic limestones overlain by a mixed siliciclastic/carbonate shoreface succession (inner to middle ramp; Fig. 9C, D). The abundant carbonaceous plant fragments in these sediments suggest adjacent tidal flats inland.
Clasts in the Guezira Formation conglomerates (see section 5.2.1) are dominated by basalt, recrystallized limestone and dolomite clasts. This composition likely reflects local provenance from the Sidi Ifni Inlier, which consists of Proterozoic igneous rocks overlain by Proterozoic-Palaeozoic carbonates (Fig. 4). Roundness, sphericity and clast composition vary along the coast. At Guezira Beach (Fig. 4) clasts tend to be more angular and are dominated by igneous clasts, whereas at Oued Craima, the conglomerates have more rounded clasts and lithologies are dominated by up to 60% carbonates. We interpret the difference in the overall clast lithology as the result of small-scale catchment areas (~100's km^2) preferentially draining igneous rocks or carbonates, in the proximity of the Ifni Inlier. The different roundness of the clasts is probably related to the mechanical stability of the main lithologies involved and not to longer transport distances/larger catchments.
In the overlying marine sandstones, clasts are dominated by quartz, although individual beds can have a significant proportion of feldspars and igneous rock fragments. Well-rounded dolomite clasts can be also present, but are not common. Quartz angularity, concentration of igneous rock fragments and feldspars and occasional dolomite clasts also points towards locally-derived sediment with relative short transport distances.
[Insert fig. 5 here]

5.2. Stratigraphy

For the purpose of comparison with other time-equivalent units in Morocco, we informally propose the subdivision of the succession into three formations (Fig. 5) easily recognizable in the field.

5.2.1. Guezira Formation

The total thickness of the unit is c. 205 m (Fig. 5). Its lower part is made of 175 m of red conglomerates and minor red sandstones unconformably overlying the Precambrian ignimbrites and andesites of the Ouarzazate Group of the Ifni Inlier (Yazidi et al., 1986). These rocks evolve into c. 8 m of dm- to m-scale fining upwards packages of red/white fine-grained sandstones with evidence of palaeosol development and

red conglomerates. The upper c. 22 m consists of dm-thick interbedded muds, fine-grained sandstones and limestones capped by a final limestone unit 1.5 m thick with abundant bioclasts, ooids and peloids. This lithostratigraphic unit is continuously exposed at Oued Craima, and stratigraphic-equivalent coarse-grained red beds have excellent lateral exposures and abundance of sedimentary structures at Guezira Beach (Fig. 4), hence the Guezira Formation is used as the name for this lower unit.

[Insert fig. 6 here]

5.2.2. Oued Craima Formation

This interval comprises ~120 m of exposed section at Oued Craima. The lower and upper contacts of this lithostratigraphic unit are not exposed. The unit starts with c. 5 m of poorly exposed red conglomerates that rapidly transitions into c. 110 m of relatively monotonous, thinly interbeded red to grey muds, fine-grained sandstones, grey oncoidal packstones, algal laminites and bioclastic- and/or peloidal-bearing mudstones/wackestones to packstones. Carbonate nodules parallel to bedding are abundant; sometimes they coalesce and form continuous beds. Occasional m-scale channelized cross-bedded bioclastic grainstones and carbonate-rich mottled palaeosols may be present. The last c. 7 m are poorly exposed coarse-grained sandstones to matrix-supported conglomerates interbedded with mud and silt, and bioturbated by dm-long vertical burrows.

[Insert fig. 7 here]

[Insert fig. 8 here]

5.2.3. Sidi Ouarzik Formation

This formation is exposed along the right bank at Oued Craima, close to the river mouth opening out into the Atlantic, and southwest of the river mouth along the beach. It is c. 217 m thick and starts with a basal c. 8 m thick unit of red conglomerates overlain by c. 16 m of interbedded fine clastics and limestones similar to the Oued Craima Fm. The succession becomes increasingly carbonate rich, with numerous dm- to m-thick interstratified units of laminated muds (and fine-grained sandstones), calcareous sandstones and bioclastic-, peloid- and ooid-bearing limestones. The upper 60–70 m of the formation show interstratified beds of hummocky cross-laminated fine-grained sandstones to silts in addition to the previous lithologies.

[Insert fig. 9 here]

5.3. Biostratigraphy

A review of previous biostratigraphic work (Choubert, 1957; Choubert et al., 1966; Benziane and Yazidi, 1982; Hollard et al., 1985; Yazidi et al., 1986; Destombes, 1991; Abou Ali et al., 2003; Benziane et al., 2016) indicates that none of the species reported in any of the previous publications provided a definitive Cretaceous age. Either the species are not diagnostic or have a broad range, extending from the Jurassic to

the Cretaceous. Identification of age-diagnostic bivalves, gastropods, foraminifera and algae in this study allows for a new biostratigraphic framework for the studied succession. The Oued Craima Formation contains an abundant macrofauna that provides a Bathonian age (Figs. 5, 10, 11). Only the lowest beds lack age-diagnostic bivalves and gastropods, with only abundant specimens of Falcimytilus sp. that could not be identified to species level. The gastropods in particular belong to a stock of species characteristic of Bathonian sediments of the Paris Basin and southern England (e.g., Lycett, 1863; Cossmann, 1885; Cox and Arkell, 1950; Cox and Maubeuge, 1950; Fischer, 1953, 1969; Fürsich et al., 1995; Fischer and Weber, 1997; for a complete list of palaeontological references see Supplementary file). A few bivalves show a wider stratigraphical and geographical distribution.

[Insert fig. 10 here]

[Insert fig. 11 here]

Long ranging foraminifera identified in thin section also give a confident Jurassic age (Mike Simmons, pers. comm.) and include *Nautiloculina oolithica* Mohler, 1938 and *Nautiloculina circularis* (Said and Barakat, 1958). A Middle to Late Jurassic age is generally accepted for those foraminifera (Kuznetsova et al., 1996; Tasli, 2001) and this age is supported by the co-occurrence of the green algae (Bruno Granier, pers. comm.) *Holosporella siamensis* (Elliott, 1983; Bassoulet, 1987; Kuss, 1990; and references therein).

The Bathonian age established in this study for the succession, makes it the oldest Mesozoic sediments exposed in the Aaiun-Tarfaya Basin to date and the most southerly Jurassic outcrops in NW Africa.

The lower ~250 m of the succession did not yield any age diagnostic fossils, including palynological analysis of the Guezira Formation. continental red beds (Fig. 4). At 205 m, foraminifer-rich grainstones yield specimens that are not age-diagnostic, but resemble Middle to Late Jurassic taxa. Conformable stratigraphic position below the confidently dated Middle Jurassic section, and sedimentologic similarity with other deposits in Morocco suggest the Guezira Formation is most likely Triassic to Lower Jurassic in age.

These new data indicate previous mis-dating of many of the Mesozoic outcrops in the Ifni area. A more likely Triassic to Middle Jurassic age (probably Bathonian) is suggested for the Mesozoic outcrops immediately surrounding the Ifni Inlier (Fig. 4).

5.4. Comparison of Jurassic stratigraphy along the Moroccan coastal basins

The recognition of Middle Jurassic deposits in the Sidi Ifni area allows a comparison of Middle Jurassic sedimentation along the Moroccan margin (Fig. 12). The margin is subdivided from south to north into the Aaiun-Tarfaya Basin, the Essaouira-Agadir Basin, and the Doukkala Basin (Figs. 1, 2).

In the Aaiun-Tarfaya Basin, the Jurassic succession exhibits a clear overall increase in thickness towards the south (Fig. 3). The thickness of Jurassic in the northern Ifni segment is up to 500 m. At Oued Craima and Sidi

Ouarzik Beach, 250–300 m of the succession is exposed and assigned to the Bathonian. In the central Tarfaya segment, the Puerto Cansado-1 well encountered a 2126 m thick Jurassic section (Martinis and Visintin, 1966; Viotti, 1966), and the Middle Jurassic recorded in the TanTan-1 well is c. 950 m thick. In the most southerly Dakhla-Boujdour segment, the thickness of the pre-Cretaceous succession has been estimated to be up to 8 km (von Rad and Einsele, 1980) with high subsidence rates, between 80 and 120 m/Ma.

In the Essaouira-Agadir Basin, facies show an overall decrease in grain size towards the northwest together with a relative increase in dolomites and anhydrites, indicative of more distal settings. In wells drilled on the present day shelf (Ghazal, 1979; Sa'd and Steyaert, 1982), the Middle Jurassic is carbonate-rich, with occasional fine clastics and minor anhydrite. Limestones range from micrite to oolitic grainstones, denoting a shallow carbonate shelf to tidal flats with occasional periods of exposure. The great areal extension of these shallow marginal marine to distal continental facies over virtually the entire basin (Amar, 1969; Le Roy et al., 1998) suggests a stable, wide, low relief basin extending over the present day shelf, covered by a shallow epicontinental sea, periodically exposed due to small eustatic or tectonic variations. Halokinesis also plays an important role, as Triassic salt diapirs were probably already active during the Middle Jurassic. The uplift of Palaeozoic terrains of the “Massif Central du Haut Atlas” to the southeast during Middle Jurassic provided the sediment delivered to the basin (Ambroggi, 1963).

In the Doukkala Basin, the Mesozoic post-rift sedimentary cover on the offshore Mazagan Plateau (Fig. 2) is much thinner than in other basins (von Rad et al., 1984), such as the Agadir-Essaouira Basin or the Aaiun-Tarfaya Basin. Middle Jurassic sediments are not exposed, but they have been penetrated by exploration wells onshore and Deep Sea Drilling Project wells offshore (Negroni et al., 1966; Hinz et al., 1982b; Le Roy et al., 1997). Sedimentary facies record an overall vertical transgression and exhibit more proximal continental-marginal marine clastic-dominated to the east and distal micritic limestones and breccias to the west (Fig. 3). The Middle Jurassic is thin in the Doukkala Basin and both the Lower and Middle Jurassic are missing towards the northeast (Figs. 2, 3).

In summary, Lower and Middle Jurassic carbonates coexist with clastics and evaporites in the northern basins (Doukkala Basin and Essaouira-Agadir Basin), while in the Aaiun-Tarfaya Basin clastic input is higher and evaporites are absent (Fig. 2). Terrigenous sedimentation during the Jurassic is not homogeneous and the northern half of the Aaiun-Tarfaya Basin seems to contain more clastic sediment (Fig. 2). The Moroccan Jurassic margin thus shows significant facies variation from north to south. This differentiation may relate to the complex inherited structure of the basement, local tectonic uplift/subsidence, variable siliciclastic input, and relative sea-level changes.

At a regional scale, published low-temperature geochronology provides data on the regional exhumation and subsidence history of the hinterland of the Western Anti-Atlas (Charton et al., 2018). Syn- and post-rift exhumation is recorded until the Middle Jurassic, which was followed by relative stability or subsidence

during the Late Jurassic and Early Cretaceous and finally resumed exhumation from the Late Cretaceous onwards.

Thickness variations and unconformities in the Aaiun-Tarfaya Basin indicate a complicated tectonic history triggered by Middle Jurassic exhumation of the Anti-Atlas and Reguibat Shield (Ruiz et al., 2011; Leprêtre, 2015; Gouiza et al., 2017, 2018; Sehrt et al., 2018) and subsidence in the basin. This complex interplay triggered a variable response in the three segments of the Aaiun-Tarfaya Basin, especially the Ifni segment. The Dakhla-Boujdour segment represents the stable, steadily subsiding distal part of the basin, progressively thinning towards the hinterland (von Rad and Einsele, 1980). This produces a tapered Jurassic sedimentary wedge opening towards the deep offshore basin (Fig. 3). The Tarfaya segment seems to have a similar evolution, with a wedge of Jurassic, although thinner and developing over a much shorter distance. This indicates less subsidence in this segment of the basin, especially during the Middle Jurassic, as the upper Lias and Dogger is only 236 m thick in the Puerto Cansado-1 well (Viotti, 1966). In the Ifni segment, during the Middle Jurassic, the presence of local unconformities and missing section in the Ifni-1 offshore well (Evans et al., 1976), relatively thick coastal sedimentary sequences and the documented exhumation of the Anti-Atlas (Charton et al., 2018), suggest increased tectonic activity that could be related to faulting and periodic uplift of this segment during the Middle Jurassic. Sedimentation occurred where accommodation developed in structural lows adjacent to the Ifni Inlier and faulted highs. The Upper Jurassic seismic sequences are continuous and thicken towards the west (Abou Ali et al., 2005), leaving a Jurassic wedge equivalent to the other segments of the Aaiun-Tarfaya Basin, although much thinner. The Jurassic thickness increase from northeast to southwest (Fig. 3) seems to be closely related with the Anti-Atlas tectonics during the Mesozoic combined with enhanced subsidence in the basin.

[Insert fig. 12 here]

5.5. Tectonic vs Eustatic Control and Timing of Western Anti-Atlas exhumation

Eustatic control on accommodation is more difficult to decipher from the sedimentary packages identified in this study. During the Bathonian, the global eustatic sea-level curve shows a gradual fall (Haq et al., 1987; Snedden and Liu, 2010). The overall deepening upwards trend observed in the sections logged records an overall increase in accommodation and relative sea-level rise/transgression. This suggests significant subsidence of the basin to accommodate the thickness of sediment and overcome the coupled effect of regional exhumation and Bathonian eustatic sea-level fall to record a deeppening/transgressive trend on the continental margin. Tectonic influence, with potential re-activation of faults along the margin, is suggested as a possible control. The Callovian unconformity in the Ifni-1 well (Evans et al., 1976) supports this and the highly subsiding domain at Craima, next to a mainly exhuming Western Anti-Atlas, has a north-south orientation that suggest a strong structural control on deposition, probably related to inherited Triassic syn-rift structures.

6. Conclusions

This study presents for the first time a detailed lithostratigraphic and depositional model for the Mesozoic sediments deposited in the Aaiun-Tarfaya Basin on the flanks of the Ifni Inlier, placed within a new biostratigraphic framework. This provides the first recorded interpretation of outcrops of Middle Jurassic and older Mesozoic sediments along this part of the NW African Central Atlantic margin. Extensive fauna (mainly bivalves and gastropods) collected and identified up to species level when possible, allows for the section exposed at Oued Craima and Sidi Ouarzik Beach to be reassigned to the Bathonian age. The age of the underlying Red Bed continental section is indeterminate at present, but its conformable relationship with the Bathonian section, suggests by superposition a Triassic to Liassic age. Sharp changes in lithology and interpreted depositional environments are easily recognizable in the field and have been used to propose for the first time in the whole Aaiun-Tarfaya Basin a subdivision in three formations for the Bathonian. (i) The Guezira Formation unconformably overlies basement. It is made of ~180 m of continental red conglomerates and minor sandstones, capped by ~20 m of peritidal and shallow marine fine clastics and carbonates. An uplifted Anti-Atlas is the sediment source. (ii) The Oued Craima Formation is ~115 m thick and mainly composed of intertidal fine sandstones, silts and microbial limestones punctuated by shallow marine lagoonal carbonates and silts. This part of the section has been confidently dated as Bathonian due to the fauna assemblages present. (iii) The Sidi Ouarzik Formation is ~190 m thick and exhibits an evolution from a thin unit of continental red conglomerates and mixed siliciclastic-carbonate tidal flats into a thick marine mixed siliciclastic-carbonate lagoon and upper-middle ramp.

The studied succession displays an overall transgressive pattern, although it was deposited during the Bathonian global eustatic sea-level fall. This signature is interpreted to record the creation of accommodation by thermal sag and tectonic subsidence overcoming the sea-level fall, punctuated by periods of coarse clastic progradation, interpreted to record short-lived local tectonics related to post-rift Anti-Atlas exhumation. Clastic input vs. carbonate production and thickness of sequences along the Aaiun-Tarfaya Basin are directly influenced by the exhumation/subsidence history of the Western Anti-Atlas. Evidence of tectonic activity ending by the early Callovian is recorded offshore near the studied area. Following this time, the stratigraphy of the basin is comparable along its length. Carbonate platforms are better developed and much thicker in the southern half of the Aaiun-Tarfaya Basin.

Tectonics and exhumation of Precambrian and Variscan domains play a key role in the early post-rift sedimentation along the Atlantic margin of Morocco. Along the Moroccan margin, mixed siliciclastic-carbonate continental to shallow marine sedimentation dominate the basins (Doukkala, Agadir-Essaouira-Agadir and the northern half of the Aaiun-Tarfaya Basin). Although the Moroccan coast is always regarded as a passive margin, inherited basement structure has controlled the distribution and style of sedimentation, with variable fill in all the coastal margin basins.

The results suggest that early post-rift sedimentary sequences deposited along the Atlantic margin of Morocco have a significant tectonic control. Inherited structures, differential subsidence rates and vertical uplift and exhumation phases in the basement terranes influenced sediment style and distribution in the basins, with eustasy playing a subordinate role. The tectonic influence reduces by the Late Jurassic when sedimentation along the Atlantic margin becomes more homogeneous and eustasy probably has a more significant control. The results have implications for the early evolution of the Central Atlantic passive margin, the controls on sedimentation and distribution of facies regionally.

Acknowledgements

This research has been possible thanks to the economic support of the sponsors within the North Africa Research Group (NARG) and logistic support in the field from ONHYM. Funding for R.G. and S.M. was provided by the University of Padova (Italy), grant GATT_SID17_01. The authors are indebted to Mike Simmons and Bruno Granier for their help with foraminifera and algae identification, and Aude Duval-Arnould, Tim Luber and Rémi Charton for their help in the field and comments on an early version of the manuscript. Pablo Corella, Arne Fuhrmann and Jianpeng Wang are thanked for their helpful discussions and assistance in the field. Stefano Castelli (University of Padova) is thanked for the photographs of gastropods and bivalves. The authors sincerely appreciate the constructive comments of Dr. M. Gouiza and Editor of Sedimentary Geology Prof. Dr. J. Knight which greatly improved the quality of the manuscript.

Appendix A. Supplementary data

Supplementary data to this article can be found online at https://doi.org/10.1016/j.sedgeo.2019.03.005.

References

Aberhan M., Bussert R., Heinrich W.-D., Schrank E., Schultkal S., Sames B. and Kapilima S., 2002. Palaeoecology and depositional environments of the Tendaguru Beds (Late Jurassic to Early Cretaceous, Tanzania). Mitteilungen aus dem Museum für Naturkunde Berlin 5, 19–44.

Abou Ali N., Chellai E.H., Nahim M. and Boudda A., 2003. Les séquences post-rift du bassin d''Ifni (Maroc atlantique): analyse de surface et de subsurface. Notes et Mémoires du Service Géologique du Maroc 452, 18–28.

Abou Ali N., Chellai E.H. and Nahim M., 2004. Anatomie d'une marge passive hybride. Marge Ifni/Tan-Tan (sud du Maroc) au Mesozoique: apports des donnees geophysiques. Estudios Geológicos 60, 111–121.

Abou Ali N., Hafid M., Chellaï E.H., Nahim M. and Zizi M., 2005. Structure de socle, sismostratigraphie et héritage structural au cours du rifting au niveau de la marge d'Ifni/Tan-Tan (Maroc sud-occidental). Comptes Rendus Geoscience 337, 1267–1276.

Alía Medina M., 1945. Características morfográficas y geológicas de la zona septentrional del Sahara español. Consejo Superior de Investigaciones Científicas, Madrid.

Alía Medina, M., 1952. Bosquejo geológico del Sahara Español. Mapa. Consejo Superior de Investigaciones Científicas, Madrid.

Allaby M. and Argyll T., 2008. Oxford Dictionary of Earth Sciences, Third. ed. Oxford University Press, New York.

Amar R., 1969. Historique du sondage Essaouira n° 1 (ESS.1). Internal report. Societe Cherifienne des Petroles, Rabat.

Ambroggi R., 1963. Étude géologique du versant méridional du Haut Atlas occidental et de la Plaine du Souss. Notes et Mémoires du Service Géologique du Maroc 157, 1–321.

Arantegui, A., 2018. Characterisation of Mesozoic Depositional Systems along the Atlantic Passive Margin of Morocco. University of Manchester, North Aaiun-Tarfaya Basin (PhD thesis).

Bailey E. and Stevens R., 1960. Selective staining of K-feldspar and plagioclase on rock slabs and thin sections. American Mineralogist 45, 1020–1025.

Bassoulet J.-P., 1987. Sarfatiella dubari Conrad & Peybernès 1973: a junior synonym of Holosporella siamensis Pia 1930. 4th International Symposium on Fossil Algae (Cardiff 6-11, July 1987), Abstracts, Friends of the Algae Newsletter, pp. 20–21.

Benziane F. and Yazidi A., 1982. Géologie de la Boutonnière précambrienne d'Ifni (Anti-Atlas occidental). Notes et Mémoires du Service Géologique du Maroc 312.

Benziane, F., Yazidi, A., Schulte, B., Boger, S., Stockhammer, S., Lehmann, A., Saadane, A., Yazidi, M., 2016. Explicative notice of the Geological map of Morocco at 1/50000, Sidi Ifni sheet. Geological Survey of Morocco n° 542 bis.

Biari Y., Klingelhoefer F., Sahabi M., Funck T., Benabdellouahed M., Schnabel M., Reichert C., Gutscher M.-A., Bronner A. and Austin J.A., 2017. Opening of the Central Atlantic Ocean: implications for geometric rifting and asymmetric initial seafloor spreading after continental breakup. Tectonics 36, 1129–1150.

Boher M., Abouchami W., Michard A., Albarede F. and Arndt N.T., 1992. Crustal Growth in West Africa at 2.1 Ga. Journal of Geophysical Research 97, 345–369.

Bouatmani R., Medina F., Ait Salem A. and Hoepffner C., 2004. Le bassin d'Essaouira (Maroc): géometrie et style des structures liées au rifting de l'Atlantique central. Africa Geoscience Review 11, 107–123.

Bradley D.C., Motts H.A., Horton J.D., Giles S. and Taylor C.D., 2015. Geologic map of Mauritania (phase V, deliverables 51a, 51b, and 51c). In: Taylor C.D., (Ed), Second Project de Renforcement Institutionnel Du Secteur Minier de La République Islamique de Mauritanie (PRISM-II). U.S. Geological Survey Open-File Report 2013-1280-A1, 3 pl., Reston, VA.

Brown R., 1980. Triassic rocks of Argana Valley, southern Morocco, and their regional structural implications. American Association of Petroleum Geologists Bulletin 64, 988–1003.

Charton R., Bertotti G., Arantegui A. and Bulot L.G., 2018. The Sidi Ifni transect across the rifted margin of Morocco (Central Atlantic): Vertical movements constrained by low-temperature thermochronology. Journal of African Earth Sciences 141, 22–32.

Choubert, G., 1957. Carte géologique du Maroc; Feuille Marrakech; Echelle: 1/500 000. Notes et Mémoires du Service Géologique du Maroc 70. Editions du Service Géologique du Maroc, Paris.

Choubert G. and Marçais J., 1956. Introduction géologique. Les grands traits de la Géologie du Maroc. Lexique Stratigraphique Du Maroc. Editions du Service Géologique du Maroc, Rabat, (168 pp.).

Choubert G., Faure-Muret A. and Hottinger L., 1966. Aperçu géologique du bassin côtier de Tarfaya. Le Bassin Côtier de Tarfaya (Maroc Méridional). Notes et Mémoires du Service Géologique du Maroc 175, Editions du Service Géologique du Maroc, Rabat (216 pp.).

Collignon M., 1966. Les céphalopodes crétacés du bassin côtier de Tarfaya: relations stratigraphiques et paléontologiques. Le Bassin Côtier de Tarfaya (Maroc Meridional). Notes et Mémoires du Service Géologique du Maroc 175. Editions du Service Géologique du Maroc, Rabat, pp. 10–149.

Cossmann M., 1885. Contribution a l'étude de la faune de l''étage bathonien en France (Gastropodes). Mémoires la Société Géologique de France, 3ème série 3, 1–374.

Cox L.R. and Arkell W.J., 1950. A survey of the Mollusca of the British Great Oolite Series. Primarily a nomenclatorial revision of the monographs by Morris and Lycett (1851–55), Lycett (1863) and Blake (1905–07). Part 2. Monograph of the Palaeontographical Society of London 103, 49–105.

Cox L.R. and Maubeuge P.-L., 1950. Révision de la faune de mollusques de l'horizon des “Stipites” du Larzac (Bathonien saumâtre). Mémoires la Société d'études paléontologiques palethnographiques Provence 2, 1–11.

Daidu F., Yuan W. and Min L., 2013. Classifications, sedimentary features and facies associations of tidal flats. Journal of Palaeogeography 2, 66–80.

Davies J.H.F.L., Marzoli A., Bertrand H., Youbi N., Ernesto M. and Schaltegger U., 2017. End-Triassic mass extinction started by intrusive CAMP activity. Nature Communications 8, 15596. https://doi.org/10.1038/ncomms15596.

Davison I., 2005. Central Atlantic margin basins of North West Africa: geology and hydrocarbon potential (Morocco to Guinea). Journal of African Earth Sciences 43, 254–274.

Destombes, J., 1991. Carte géologique du Maroc, feuille au 1/100000, Tiznit. Notes et Mémoires du Service Géologique du Maroc 360.

Dickson J., 1966. Carbonate identification and genesis as revealed by staining. Journal of Sedimentary Research 36, 491–505.

du Dresnay R., 1988. Répartition des dépôts carbonatés du Lias inférieur et moyen le long dela côte atlantique du Maroc: conséquences sur la paléogéographie del'Atlantique naissant. Journal of African Earth Sciences 7, 385–396.

Echarfaoui H., Hafid M., Aït Salem A. and Abderrahmane A.F., 2002. Analyse sismo-stratigraphique du bassin d'Abda (Maroc occidental), exemple de structures inverses pendant le rifting atlantique. Comptes Rendus Geoscience 334, 371–377.

Einsele G. and von Rad U., 1979. Facies and paleoenvironment of Lower Cretaceous sediments at DSDP Site 397 and in the Aaiun Basin (Northwest Africa). In: von Rad U. and Ryan W.B.F., (Eds.), Initial Reports of the Deep Sea Drilling Project, v 47, Part 1. Texas A & M University, Ocean Drilling Program, College Station, TX, United States, pp. 559–571.

El Jorfi L., Süss M.P., Aigner T. and Mhammdi N., 2015. Triassic-Quaternary Sequence Stratigraphy of the Tarfaya Basin (Moroccan Atlantic): Structural evolution, Eustasy and Sedimentation. Journal of Petroleum Geology 38, 77–98.

El Khatib J., Ruellan É., El Foughali A. and El Morabet A., 1995. Évolution de la marge atlantique sud marocaine: bassin de Tarfaya-Laâyoune. Comptes Rendues, Académie des sciences Paris, Sciences de la Terre et des Planètes 320, 117–124.

El Khatib J., El Foughali A., Ruellan É. and El Morabet A., 1996. Évolution post-rift des secteurs NE et SW du bassin Tarfaya-Laâyoune. Mines, Géologie et Energie 55, 57–72.

Elbatal Y., Aadjour M., Saber N., Elabibi R. and Nahim M., 2010. Étude sismo-structurale du bassin de Tarfaya-Boujdour Onshore. Afrique Science 06, 49–59.

Elliott G.F., 1983. Distribution and affinities of the Jurassic dasycladalean alga Sarfatiella. Palaeontology 26, 671–675.

Evans D.J., Fisher M.J., Haskins C.W. and Laing J.F., 1976. Biostratigraphy and depositional environments of the interval 729’ to 6560’ TD in the Sun Oil Company Ifni No. 1 well offshore South-West Morocco. Internal report, Maroc Sun Oil Company.

Fischer J.-C., 1953. Notes sur les gastéropodes d'un niveau gîte coquillier du Bathonien des Ardennes. Journal de Conchyliologie 93, 3–25.

Fischer J.-C., 1969. Géologie, paléontologie et paléoécologie du Bathonien en sud-ouest du Massiv Ardennais. Mémoires du Muséum National d'Histoire Naturelle de Paris (Série C) 20, 1–319.

Fischer J.-C. and Weber C., 1997. Révision critique de la Paléontologie Française d'Alcide d'Orbigny (incluant la réédition de l'original). Volume II, gastropodes jurassiques. Muséum National d'Histoire Naturelle and Masson, Paris, (300 pp.).

Flügel E., 2010. Microfacies of Carbonate Rocks: Analysis, Interpretation and Application. 2nd ed., Springer, Berlin Heidelberg.

Frizon De Lamotte D., Zizi M., Missenard Y., Hafid M., El Azzouzi M., Maury R.C., Charrière A., Taki Z., Benammi M. and Michard A., 2008. The Atlas System. In: Michard A., Saddiqi O., Chalouan A. and Frizon De Lamotte D., (Eds.), Continental Evolution, The Geology of Morocco. Springer Verlag, Berlin Heidelberg, pp. 133–202.

Frizon de Lamotte D., Leturmy P., Missenard Y., Khomsi S., Ruiz G., Saddiqi O., Guillocheau F. and Michard A., 2009. Mesozoic and Cenozoic vertical movements in the Atlas system (Algeria, Morocco, Tunisia): an overview. Tectonophysics 475, 9–28.

Fürsich F.T., Freytag S., Röhl J. and Schmid A., 1995. Palaeoecology of benthic associations in salinity-controlled marginal marine environments: examples from the Lower Bathonian (Jurassic) of the Causses (southern France). Palaeogeography, Palaeoclimatology, Palaeoecology 113, 135–172.

Ghazal R.L., 1979. Cap-Sim 1X well. Final Geological Report. Confidential report.

Ginsburg R.N., Hardie L.A., Bricker O.P., Garrett P. and Wanless H., 1977. Exposure index: A quantitative approach to defining position within the Tidal Zone. In: Hardie L.A., (Ed), Sedimentation on the Modern Carbonate Tidal Flats of Northwest Andros Island, Bahamas. Johns Hopkins University Press, Baltimore, pp. 7–12.

Gouiza M., 2011. Mesozoic Source-to-Sink Systems in NW Africa: Geology of vertical movements during the birth and growth of the Moroccan rifted margin, (PhD thesis), VU University Amsterdam.

Gouiza M., Charton R., Bertotti G., Andriessen P. and Storms J.E.A., 2017. Post-Variscan evolution of the Anti-Atlas belt of Morocco constrained from low-temperature geochronology. International Journal of Earth Sciences 106, 593–616.

Gouiza M., Bertotti G. and Andriessen P.A.M., 2018. Mesozoic and Cenozoic thermal history of the Western Reguibat Shield (West African Craton). Terra Nova 30, 135–145.

Gradstein F.M., Ogg J.G. and Hilgen F.J., 2012. On the Geologic Time Scale. Newsletters on Stratigraphy 45, 171–188.

Hafid M., 2000. Triassic-early Liassic extensional systems and their Tertiary inversion, Essaouira Basin (Morocco). Marine and Petroleum Geology 17, 409–429.

Hafid M., Salem A.A. and Bally A.W., 2000. The western termination of the Jebilet High- Atlas system (Offshore Essaouiara Basin, Morocco). Marine and Petroleum Geology 17, 431–443.

Hafid M., Zizi M., Bally A.W. and Ait Salem A., 2006. Structural styles of the western onshore and offshore termination of the High Atlas, Morocco. Comptes Rendus Geoscience 338, 50–64.

Hafid M., Tari G.C., Bouhadioui D., El Moussaid I., Echarfaoui H., Aït Salem A., Nahim M. and Dakki M., 2008. Atlantic Basins. In: Michard A., (Ed), Continental Evolution. The Geology of Morocco. Springer, Berlin Heidelberg, pp. 303–329.

Haq B.U., Hardenbol J. and Vail P.R., 1987. Chronology of fluctuating sea levels since the Triassic. Science 235, 1156–1167.

Hardie L.A., 1977. Sedimentation on the Modern Carbonate Tidal Flats of Northwest Andros Island. Johns Hopkins University Press, Bahamas (202 pp.).

Hardie L.A., 1986. Stratigraphic models for tidal deposition. In: Hardie L.A. and Shinn E.A., (Eds.), Carbonate Depositional Environments, Modern and Ancient. Colorado School of Mines, pp. 59–74.

Hinz K., Dostmann H. and Fritsch J., 1982a. The continental margin of Morocco: Seismic sequences, structural elements and geological development. In: von Rad U., Hinz K., Sarnthein M. and Seibold E., (Eds.), Geology of the Northwest African Continental Margin. Springer, Berlin Heidelberg, pp. 34–60.

Hinz K., Winterer E.L., Baumgartner P.O., Bradshaw M.J., Channell J.E.T., Jaffrezo M., Jansa L.F., Leckie R.M., Moore J.N., Rullkötter J., Schaftenaar C., Steiger T.H., Vuchev V. and Wiegand G.E., 1982b. Preliminary results from DSDP Leg 79 seaward of the Mazagan Plateau off Central Morocco. In: von Rad U., Hinz K., Sarnthein M. and Seibold E., (Eds.), Geology of the Northwest African Continental Margin. Springer Verlag, Berlin Heidelberg New York, pp. 23–33.

Hollard, H., Choubert, G., Bronner, G., Marchand, J., Sougy, J.M.A., 1985. Carte géologique du Maroc; Echelle: 1/1000 000. Notes et Mémoires du Service Géologique du Maroc 260.

Jansa L.F. and Wiedmann J., 1982. Mesozoic-Cenozoic development of the Eastern north American and Northwest African continental margins: A comparison. In: von Rad U., Hinz K., Sarnthein M. and Seibold E., (Eds.), Geology of the Northwest African Continental Margin. Springer Verlag, Berlin Heidelberg New York, pp. 215–269.

Klitgord K.D. and Schouten H., 1986. Plate kinematics of the Central Atlantic. In: Vogt P.R. and Tucholke B.E., (Eds.), The Geology of North America, Volume M, The Western North Atlantic Region. Geological Society of America, pp. 351–378.

Kuss J., 1990. Middle Jurassic Calcareous Algae from the Circum-Arabian Area. Facies 22, 59–85.

Kuznetsova K.K., Grigelis A., Adjamian J. and Hallaq L., 1996. Zonal Stratigraphy and Foraminifera of the Tethyan Jurassic (Eastern Mediterranean). Gordon & Breach Science, Amsterdam.

Labails C., Olivet J.-L., Aslanian D. and Roest W.R., 2010. An alternative early opening scenario for the Central Atlantic Ocean. Earth and Planetary Science Letters 297, 355–368.

Lancelot Y. and Winterer E.L., 1980. Evolution of the Moroccan oceanic basin and adjacent continental margin—A synthesis. In: Stout L.N. and Worstell P., (Eds.), Initial Reports of the Deep Sea Drilling Project 50, U.S. Government Printing Office, Washington, pp. 801–821.

Le Roy P., Piqué A., Le Gall B., Ait Brahim L., Morabet A.M. and Demnati A., 1997. Les bassins cotiers triasico-liasiques du Maroc occidental et la diachronie du rifting intra-continental de l'Atlantique central. Bulletin de la Société Géologique de France 168, 637–648.

Le Roy P., Guillocheau F., Piqué A. and Morabet A.M., 1998. Subsidence of the Atlantic Moroccan margin during the Mesozoic. Canadian Journal of Earth Sciences 35, 476–493.

Leprêtre R., 2015. Evolution phanérozoïque du Craton Ouest Africain et de ses bordures Nord et Ouest, (PhD thesis), Université Paris Sud.

Leprêtre R., Barbarand J., Missenard Y., Leparmentier F. and Frizon de Lamotte D., 2013. Vertical movements along the northern border of the West African Craton: the Reguibat Shield and adjacent basins. Geological Magazine 151, 885–898.

Luber T.L., Bulot L.G., Redfern J., Frau C., Arantegui A. and Masrour M., 2017. A revised ammonoid biostratigraphy for the Aptian of NW Africa: Essaouira-Agadir Basin, Morocco. Cretaceous Research 79, 12–34.

Lycett J., 1863. Supplementary monograph on the Mollusca from the Stonefield Slate, Great Oolite, Forest Marble, and Cornbrash. Monograph of the Palaeontographical Society of London 15, 1863, 1–129.

Martinis B. and Visintin V., 1966. Données géologiques sur le bassin sédimentaire côtier de Tarfaya (Maroc méridional). In: Reyre D., (Ed), Bassin Sedimentaires Du Littoral Africain. Union Internationale des Sciences Géologiques, Paris, pp. 13–26.

Meddah A., Bertrand H., Seddiki A. and Tabeliouna M., 2017. The Triassic-Liassic volcanic sequence and rift evolution in the saharan atlas basins (Algeria). Eastward vanishing of the central Atlantic magmatic province. Geologica Acta 15, 11–23.

Medina F., 1995. Syn- and postrift evolution of the El Jadida-Agadir basin (Morocco): constraints for the rifting model of the Central Atlantic. Canadian Journal of Earth Sciences 32, 1273–1291.

Meyer D.E., 1978. Microfacies and microfabrics of early Middle Cretaceous sediments selected from Site 370, DSDP Leg 41 (deep basin off Morocco). Initial Reports of the Deep Sea Drilling Project; Supplement to Volumes XXXVIII, XXXIX, XL, and XLI, pp. 961–981.

Michard A., Frizon de Lamotte D., Liégeois J.-P., Saddiqi O. and Chalouan A., 2008a. Conclusion: Continental Evolution in Western Maghreb. In: Michard A., Saddiqi O., Chalouan A. and Frizon de Lamotte D., (Eds.), Continental Evolution: The Geology of Morocco. Structure, Stratigraphy, and Tectonics of the Africa-Atlantic-Mediterranean Triple Junction. Springer Verlag, Berlin Heidelberg, pp. 395–404.

Michard A., Saddiqi O., Chalouan A. and Frizon de Lamotte D., 2008b. Continental evolution: The geology of Morocco. In: Structure, Stratigraphy, and Tectonics of the Africa-Atlantic-Mediterranean Triple Junction. Springer Verlag, Berlin Heidelberg, (424 pp.).

Mulder T., Syvitski J.P.M., Migeon S., Faugères J.C. and Savoye B., 2003. Marine hyperpycnal flows: Initiation, behaviorand related deposits. A review. Marine and Petroleum Geology 20, 861–882.

Negroni P., Gendrot C. and Jahn Skwirblies, 1966. Forage de reconnaissance OLD 1 A (Oualidia 1 A). Rapport geologique et technique. Internal Report, Preussag-Maroc.

Price I., 1980. Provenance of the Jurassic-Cretaceous flysch, deep sea drilling project sites 370 and 416. Initial Reports of the Deep Sea Drilling Project 50, 751–757.

Querol R., 1966. Regional geology of the Spanish Sahara. In: Reyre D., (Ed), Bassins Sédimentaires Du Littoral Africain. Association des Services Géologiques Africains, New Delhi, pp. 27–39.

Ruiz G.M.H., Sebti S., Negro F., Saddiqi O., Frizon de Lamotte D., Stockli D., Foeken J., Stuart F., Barbarand J. and Schaer J.P., 2011. From central Atlantic continental rift to Neogene uplift - western Anti-Atlas (Morocco). Terra Nova 23, 35–41.

Sa'd J. and Steyaert D.J., 1982. Essaouira 1X final well report. Part I, Geology. Internal Report. Phillips Petroleum Company.

Sahabi M., Aslanian D. and Olivet J.-L., 2004. Un nouveau point de départ pour l'histoire de l'Atlantique central. Comptes Rendus Geoscience 336, 1041–1052.

Said R. and Barakat M.G., 1958. Jurrasic Microfossils from Gebel Maghara, Sinai, Egypt. Micropaleontology 4, 231–272.

Schettino A. and Turco E., 2009. Breakup of Pangaea and plate kinematics of the central Atlantic and Atlas regions. Geophysical Journal International 178, 1078–1097.

Schlüter T., 2006. Geological Atlas of Africa: With Notes on Stratigraphy, Tectonics, Economic Geology, Geohazard and Geosites of Each Country, Geological Atlas of Africa. Springer Verlag, Berlin Heidelberg.

Scotese C.R., 1991. Jurassic and cretaceous plate tectonic reconstructions. Palaeogeography, Palaeoclimatology, Palaeoecology 87, 493–501.

Sehrt M., Glasmacher U.A., Stockli D.F., Jabour H. and Kluth O., 2018. The southern Moroccan passive continental margin: an example of differentiated long-term landscape evolution in Gondwana. Gondwana Research 53, 129–144.

Seibold E., 1982. The northwest African continental margin. In: von Rad U., Hinz K., Sarnthein M. and Seibold E., (Eds.), Geology of the Northwest African Continental Margin. Springer Verlag, Berlin Heidelberg New York, pp. 3–20.

Snedden J.W. and Liu C., 2010. A Compilation of Phanerozoic Sea-Level Change, Coastal Onlaps and Recommended Sequence Designations. American Association of Petroleum Geologists, Search and Discovery Article 40594, 2004–2006. https://doi.org/10.1167/iovs.08-2844.

Spence G.H. and Tucker M.E., 2007. A Proposed integrated multi-signature model for peritidal cycles in carbonates. Journal of Sedimentary Research 77, 797–808.

Steiner C., Hobson A., Favre P., Stampfli G.M. and Hernandez J., 1998. Mesozoic sequence of Fuerteventura (Canary Islands): witness of Early Jurassic sea-floor spreading in the central Atlantic. Geological Society of America Bulletin 110, 1304–1317.

Tari G.C. and Jabour H., 2013. Salt tectonics along the Atlantic margin of Morocco. In: Mohriak W.U., Danforth A., Post P.J., Brown D.E., Tari G.C., Nemčok M. and Sinha S.T., (Eds.), Conjugate Divergent Margins. Geological Society, London, Special Publications, pp. 337–353.

Tari G.C., Jabour H., Molnar J., Valasek D. and Zizi M., 2012. Deep-water exploration in Atlantic Morocco. In: Gao D., (Ed), Tectonics and Sedimentation: Implications for Petroleum Systems. American Association of Petroleum Geologists Special Publications, Memoir vol. 100, pp. 337–355.

Tasli K., 2001. Benthic Foraminifera of the Upper Jurassic Platform Carbonate Sequence in the Aydincik (Içel) Area, Central Taurides, S Turkey. Geologica Croatica 54, pp. 1–13.

van Houten F.B., 1977. Triassic-Liassic deposits of Morocco and Eastern North America: comparison. American Association of Petroleum Geologists Bulletin 61, 79–99.

Villeneuve M., 2005. Paleozoic basins in West Africa and the Mauritanide thrust belt. Journal of African Earth Sciences 43, 166–195.

Viotti C., 1965. Microfaunes et microfaciès du sondage Puerto Cansado 1 (Maroc méridional, province de Tarfaya). Mémoire Bureau de Recherches Géologiques et Minière. Colloque International de Micropaléontologie. Dakar 32, pp. 29–40.

Viotti C., 1966. Resultats stratigraphiques du sondage Puerto Cansado 1 du bassin cotier de Tarfaya. Notes et Mémoires du Service Géologique du Maroc 175. Editions du Service Géologique du Maroc, Rabat.

von Rad U. and Einsele G., 1980. Mesozoic-Cainozoic Subsidence history and Palaeobathymetry of the Northwest African Continental Margin (Aaiun Basin to D. S. D. P. Site 397). Philosophical Transactions of the Royal Society A: Mathematical, Physical and Engineering Sciences 294, 37–50.

von Rad U. and Wissmann G., 1982. Cretaceous-Cenozoic history of the West Saharan continental margin (NW Africa): development, destruction and gravitational sedimentation. In: von Rad U., Hinz K., Sarnthein M. and Seibold E., (Eds.), Geology of the Northwest African Continental Margin. Springer, Berlin Heidelberg, pp. 106–131.

von Rad U., Čepek P., von Stackelberg U., Wissmann G. and Zobel B., 1979. Cretaceous and Tertiary sediments from the Northwest African slope (dredges and cores supplementing DSDP results). Marine Geology 29, 273–312.

von Rad U., Auzende J.-M., Ruellan É. and Group, C, 1984. Stratigraphy, structure, paleoenvironment and subsidence history of the Mazagan Escarpment off central Morocco: a synthesis of the results of the CYAMAZ deep diving expedition. Oceanologica Acta Special Volume 5, 161–182.

Wenke A.A.O., 2015. Sequence stratigraphy and basin analysis of the Meso- to Cenozoic Tarfaya- Laâyoune Basins, on- and offshore Morocco, (PhD thesis). Ruprecht-Karls-Universität Heidelberg.

Wenke A.A.O., Zühlke R., Jabour H. and Kluth O., 2011. High-resolution sequence stratigraphy in basin reconnaissance: example from the Tarfaya Basin, Morocco. First Break 29, 2011, 85–96.

Wilson M. and Guiraud R., 1998. Late Permian to Recent magmatic activity on the African-Arabian margin of Tethys. In: Macgregor D.S., Moody R.T.J. and Clark-Lowes D.D., (Eds.), Petroleum Geology of North Africa. Geological Society, London, Special Publications No. 132, pp. 231–263.

Winterer E.L. and Hinz K., 1984. The evolution of the Mazagan Continental margin: a synthesis of geophysical and geological data with results of drilling during DSDP leg. 79. Initial Reports of the Deep Sea Drilling Project 79, pp. 893–919.

Wright V.P., 1983. Morphogenesis of Oncoids in the Lower Carboniferous Llanelly Formation of South Wales. In: Peryt T.M., (Ed), Coated grains. Springer-Verlag, pp. 424–434.

Wright V.P., 1984. Peritidal carbonate facies models: a review. Geological Journal 19, 309–325.

Yazidi, A., Benziane, F., Hollard, H., Destombes, J., Oliva, P., 1986. Carte géologique du Maroc, feuille au 1/100000, Sidi Ifni. Notes et Mémoires du Service Géologique du Maroc n° 310. Editions du Service Géologique du Maroc, Rabat.

Zühlke R., Bouaouda M.S., Ouajhain B., Bechstädt T. and Leinfelder R., 2004. Quantitative Meso-/Cenozoic development of the eastern Central Atlantic continental shelf, western High Atlas, Morocco. Marine and Petroleum Geology 21, 225–276.

FIGURE CAPTIONS

Fig. 1. Simplified geological map of north-west Africa showing the main structural elements around the Aaiun-Tarfaya Basin. Compiled after Hollard et al. (1985); Boher et al. (1992); Davison (2005); Villeneuve (2005); Schlüter (2006); Michard et al. (2008a); Frizon de Lamotte et al. (2009); Leprêtre et al. (2013); Bradley et al. (2015) and Meddah et al. (2017). RB: Rharb Basin. DB: Doukkala Basin. EAB: Essaouira-Agadir Basin.For consistency throughout the text the order of the names in the Essaouira-Agadir Basin (EAB) have been rearranged.

Fig. 2. Generalised chronostratigraphy of basins along the Atlantic Margin of Morocco (see Fig. 1 for location). From north to south: Doukkala Basin adapted after Negroni et al. (1966); Meyer (1978); Lancelot and Winterer (1980); Price (1980); Winterer and Hinz (1984) and Echarfaoui et al. (2002). Agadir-Essaouira Basin offshore stratigraphy adapted after Hafid et al. (2000); Tari et al. (2012) and unpublished well report; onshore stratigraphy adapted after Hafid (2000); Luber et al. (2017); Aaiun-Tarfaya Basin - Ifni segment offshore stratigraphy adapted after Abou Ali et al. (2005) and Gouiza (2011); onshore stratigraphy from this study. Aaiun-Tarfaya Basin - Tarfaya segment offshore stratigraphy adapted after Wenke (2015); onshore stratigraphy adapted after Hollard et al. (1985) and Arantegui (2018). Aaiun-Tarfaya Basin - Boujdour-Dakhla segment adapted after von Rad and Einsele (1980); von Rad and Wissmann (1982). Time scale after Gradstein et al. (2012). Numbers to the right of each basin represent the most important formations as follows: (1) Jreibichat Fm., (2) Lebtaina Fm., (3) Samlat Fm., (4) Aaiun Fm., (5) Puerto Cansado Fm., (6) Tan Tan Fm., (7) Aguidir Fm., (8) Tah Fm., (9) Hammada Tellia Fm., (10) Ikakern Fm., (11) Timezgadiwine Fm., (12) Bigoudine Fm., (13) Amsittene Fm., (14) Id Ou Moulid Fm., (15) Ameskhoud Fm., (16) Ouanamane Fm., (17) Tidili Fm., (18) Imouzzer Fm., (19) Tismeroura Fm., (20) Cap Tafalney Fm., (21) Sidi Lhouseine Fm., (22) Tamanar Fm., (23) Bouzergoun Fm., (24) Tamzergout Fm., (25) Oued Tidzi Fm., (26) Calcaire de Dridat Fm.

Fig. 3. Schematic dip cross-sections showing the architecture of Moroccan coastal basins. From north to south: (A) Doukkala Basin, adapted after Hinz et al. (1982a, 1982b); Hollard et al. (1985) and Le Roy et al. (1997). (B) Agadir-Essaouira Basin adapted after Hafid (2000); Frizon De Lamotte et al. (2008); Tari and Jabour (2013). (C) Aaiun-Tarfaya Basin (Ifni segment) adapted after Abou Ali et al. (2005) and Hafid et al. (2008). (D) Aaiun-Tarfaya basin (Tarfaya segment) adapted after Hinz et al. (1982a, 1982b); Abou Ali et al. (2005) and Wenke et al. (2011). (E) Aaiun-Tarfaya basin (Boujdour-Dakhla segment) adapted after von Rad et al. (1979); von Rad and Einsele (1980); Hollard et al. (1985); Hafid et al. (2008).

Fig. 4. Geology of the Ifni Inlier and surroundings simplified after Choubert (1957); Yazidi et al. (1986) and Destombes (1991). GB: Guezira Beach. IP: Ifni Port.

Fig. 5. Summary stratigraphic log of Craima, including proposed formation names, individual parasequences, systems tracts and main macrofauna. Lithologies as in Fig. 2.

Fig. 6. Examples from the field and microphotographs of alluvial fans and alluvial floodplain facies associations. Lithology and symbols as in Figs. 2, 5. (A) Field panorama showing alternating packages of red conglomerates and fine sandstones belonging to FA1 and FA2 (see text for details). (B) Detail of sedimentary log collected in the field. Note the current-generated sedimentary structures are localised in the coarser sandstone levels. (C) Field picture of palaesols developed in fine-grained sandstones. Rootlet marks are visible. Hammer is 33 cm long. (C) Microphotograph from the white sandstone level in 2a (upper half in plane polarised light and lower half in cross polarised light). (E, F) Field picture of conglomeratic beds, and microphotograph of the matrix (upper half in plane polarised light and lower half in cross polarised light). Stick for scale is 1.2 m long. Qtz: detrital quartz; fd: detrital feldspar.

Fig. 7. Example of a typical peritidal parasequence. Lithology and symbols as in Figs. 2, 5. (A) Field overview of a shallowing-upwards peritidal parasequence of cross-bedded grainstones overlain by silts and fine sandstones, capped by the next channelised coarse sandstone. Note the ostracods-rich limestone below the first cross-bedded grainstone/calcareous sandstone represents the base of a progradational parasequence. (B) Annotated log from the field (each black/white bar represents 1 m). (C, D, G, H) Examples of lithofacies O. (E, F) Mottled palaeosols developed on fine-grained sandstones. Qtz: detrital quartz; fd: detrital feldspar.

Fig. 8. Examples of lagoonal facies (FA4 and FA5) along Sidi Ouarzik Beach outcrop. (A) Field panorama showing several shoaling-upwards cycles. (B) Detailed field sedimentary log. Black/white bars represent 1 m. Lithology and symbols as in Figs. 2, 5. (C, D) Field view and microphotograph of silty bioclastic-bearing mudstones/wackestones. Main bioclasts are bivalves (*Dacryomya* cf. *lacrima*, *Myophorella tuberculosa*, *Eocallista antiopa*) gastropods (*Nerinella*? sp.) and minor unidentified ostracods. (E) Field example of top surface completely dissected by dewatering structures. Stick is 1.2 m long. (F) Microphotograph showing green algae fragments (*Holosporella siamensis*, Pia 1930) as main bioclast. Silt-graded detrital quartz (qtz) is abundant in this silty bioclastic packstone. (G) Closer view of coarsening- and shallowing-upwards parasequences of laminated to thinly bedded muds passing into fine sandstones (sometimes bioclastic). (H) Another example of muds overlain by sandstones. Stick in the field of view is 90 cm long, and each subdivision is 10 cm.

Fig. 9. Depositional model illustrating the main four stages in the evolution of the system. (A) Triassic/Liassic deposition of red alluvial fans directly fed from the Ifni Inlier to the east. (B) Development of a peritidal coastal plain characterised by the interplay between terigenous clastics supplied from the Ifni Inlier and the coastal processes (mainly tides). This stage in the evolution of the system can be confidently dated as Bathonian based on the analysed fauna. (C) The coastal plain gets drowned and a shallow lagoon is established where fine-grained clastics and carbonate production coexist. (D) Marine sedimentation continues and the system becomes slightly coarser and siliciclastic-rich. Bathonian fauna still can be found during this stage.

Fig. 10. Bivalves identified in the succession. See Supplementary material for additional information on stratigraphic and geographic distribution. 1 - *Dacryomya* cf. *lacrima* (J. de C. Sowerby, 1824), 2 - *Falcimytilus* sp., 3 - *Costigervillia* sp., 4 - *Isognomon isognomonoides* (Stahl, 1824), 5 - *Placunopsis socialis* Morris & Lycett, 1853, 6a, 6b - *Trigonia pullus* J. de C. Sowerby, 1826, 7 - *Myophorella tuberculosa* (Lycett, 1850), 8 - *Nicaniella pulla* (Roemer, 1836), 9 - *Protocardia lycetti* (Rollier, 1912), 10a, 10b - *Pronoella* sp., 11 - *Eocallista antiopa* (d'Orbigny, 1850), 12 - *Eomiodon angulatus* (Morris & Lycett, 1855), 13 - "*Corbula*" cf. *involuta* Münster in Goldfuss, 1837, 14 - *Pachyrisma grande* Morris & Lycett, 1850, 15 - *Ceratomya concentrica* (J. de C. Sowerby, 1825).

Fig. 11. Gastropods identified in the succession. See Supplementary material for additional information on stratigraphic and geographic distribution. 1 - Zygopleuridae indet., 2 - *Pseudomelania* (*Oonia*) *variata* (Lycett, 1863), 3 - *Eligmoloxus limneiformis* Cossmann, 1885, 4 - *Exelissa* cf. *binodosa* Grundel, 1990, 5 - *Cryptaulax* sp., 6, 7a, 7b - *Globularia* cf. *eparcyensis* (d'Archiac, 1843), 8 - *Globularia* cf. *tancredi* (Morris & Lycett, 1850), 9 - *Ampullospira actaea* (d'Orbigny, 1850), 10 - *Globularia* sp., 11a, 11b - *Naricopsina matheroni* (Gourret, 1884), 12 - *Pictavia*? cf. *stricklandi* (Morris & Lycett, 1850), 13 - *Phaneroptyxis*? sp., 14 - *Nerinella elegantula* (d'Orbigny, 1850), 15, 16, 17, 17a - *Ceritella dewalquei* (Piette, 1857), 18 - *Sinuarbullina*? sp.

Fig. 12. Palaeoenvironmental reconstruction along the Moroccan Atlantic margin for the Bathonian. Jurassic shelf after Hinz et al. (1982a, 1982b); Seibold (1982) and Hafid et al. (2006). Shoreline in the Doukkala and Agadir-Essaouira Basins after Medina (1995).

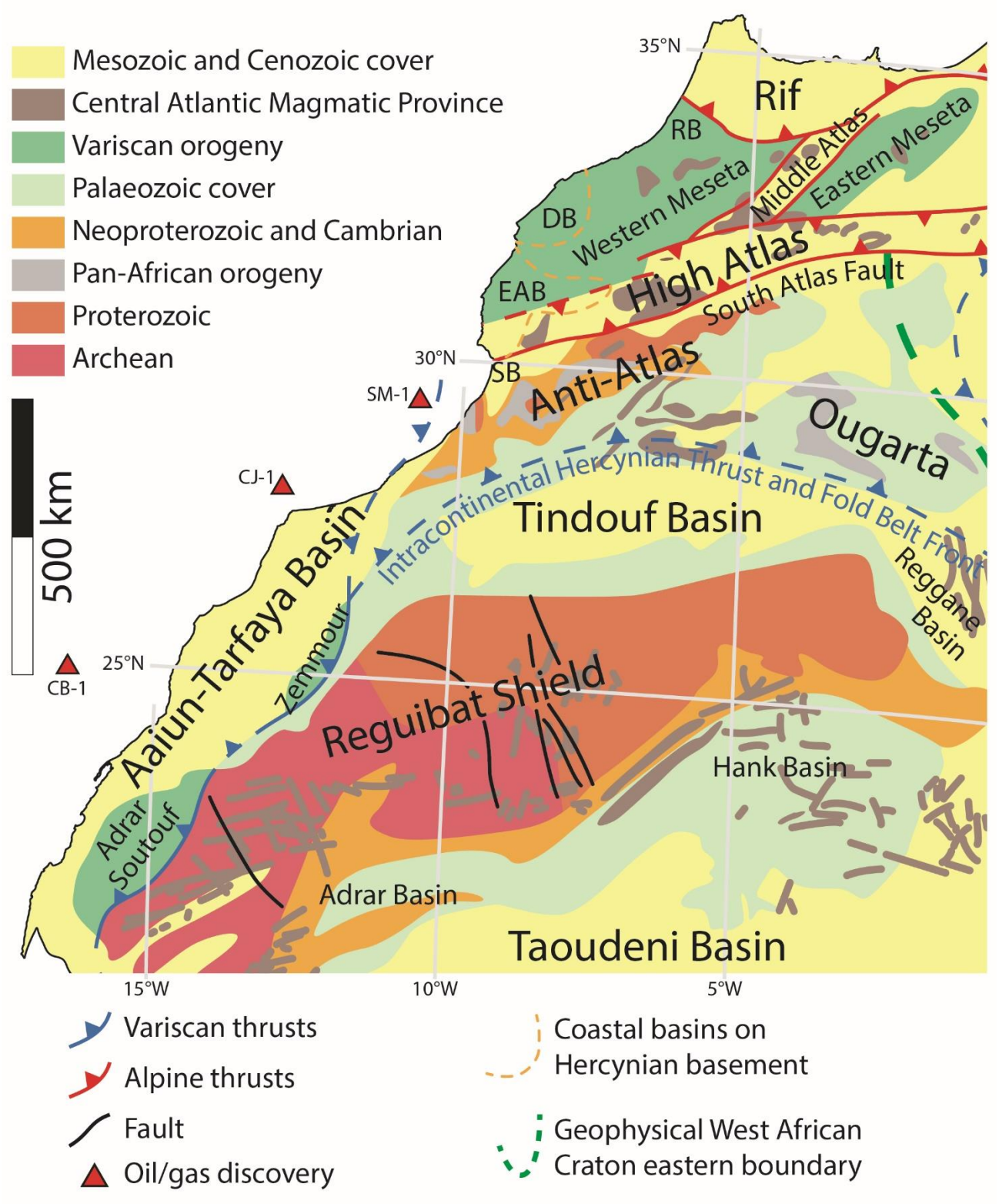
Mesozoic and Cenozoic cover
Central Atlantic Magmatic Province
Variscan orogeny
Palaeozoic cover
Neoproterozoic and Cambrian
Pan-African orogeny
Proterozoic
Archean
500 km
35°N
30°N
25°N
15°W
10°W
5°W
Rif
RB
Western Meseta
Middle Atlas
Eastern Meseta
DB
EAB
High Atlas
South Atlas Fault
SB
Anti-Atlas
SM-1
CJ-1
CB-1
Ougarta
Intracontinental Hercynian Thrust and Fold Belt Front
Tindouf Basin
Reggane Basin
Aaiun-Tarfaya Basin
Zemmour
Reguibat Shield
Hank Basin
Adrar Soutouf
Adrar Basin
Taoudeni Basin
Variscan thrusts
Alpine thrusts
Fault
Oil/gas discovery
Coastal basins on Hercynian basement
Geophysical West African Craton eastern boundary

Fig. 1

Fig. 2

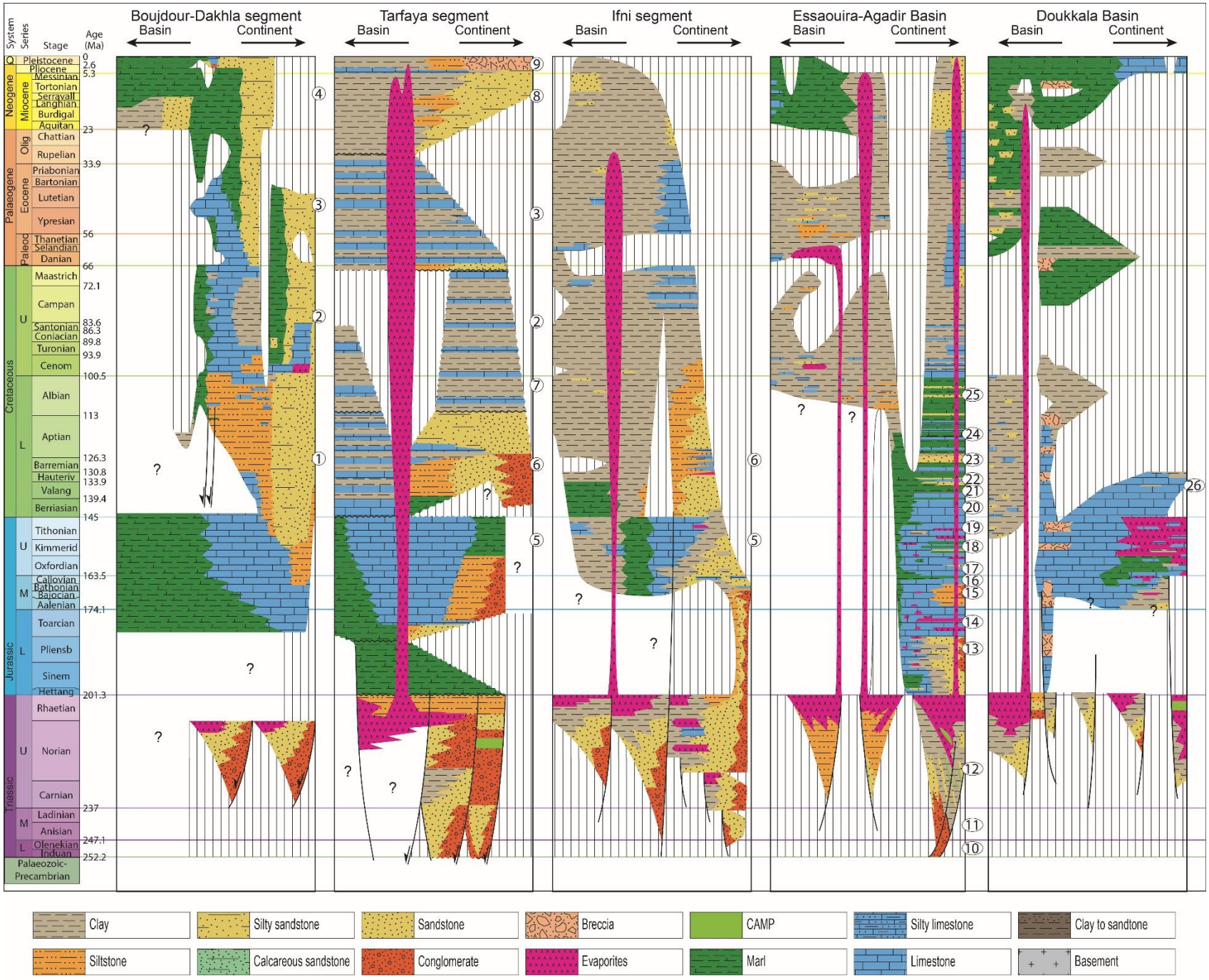
System
Series
Stage
Age (Ma)
Boujdour-Dakhla segment
Basin
Continent
Tarfaya segment
Basin
Continent
Ifni segment
Basin
Continent
Essaouira-Agadir Basin
Basin
Continent
Doukkala Basin
Basin
Continent
Q
Pleistocene
Pliocene
Neogene
Miocene
Messinian
Tortonian
Serravall
Langhian
Burdigal
Aquitan
23
Olig
Chattian
Rupelian
33.9
Palaeogene
Eocene
Priabonian
Bartonian
Lutetian
Ypresian
56
Paleoc
Thanetian
Selandian
Danian
66
Cretaceous
U
Maastrich
72.1
Campan
83.6
Santonian
86.3
Coniacian
89.8
Turonian
93.9
Cenom
100.5
L
Albian
113
Aptian
126.3
Barremian
130.8
Hauteriv
133.9
Valang
139.4
Berriasian
145
Jurassic
U
Tithonian
Kimmerid
Oxfordian
163.5
M
Callovian
Bathonian
Bajocian
Aalenian
174.1
L
Toarcian
Pliensb
Sinem
Hettang
201.3
Triassic
U
Rhaetian
Norian
Carnian
237
M
Ladinian
Anisian
247.1
L
Olenekian
Induan
252.2
Palaeozoic-Precambrian
Clay
Silty sandstone
Sandstone
Breccia
CAMP
Silty limestone
Clay to sandtone
Siltstone
Calcareous sandstone
Conglomerate
Evaporites
Marl
Limestone
Basement

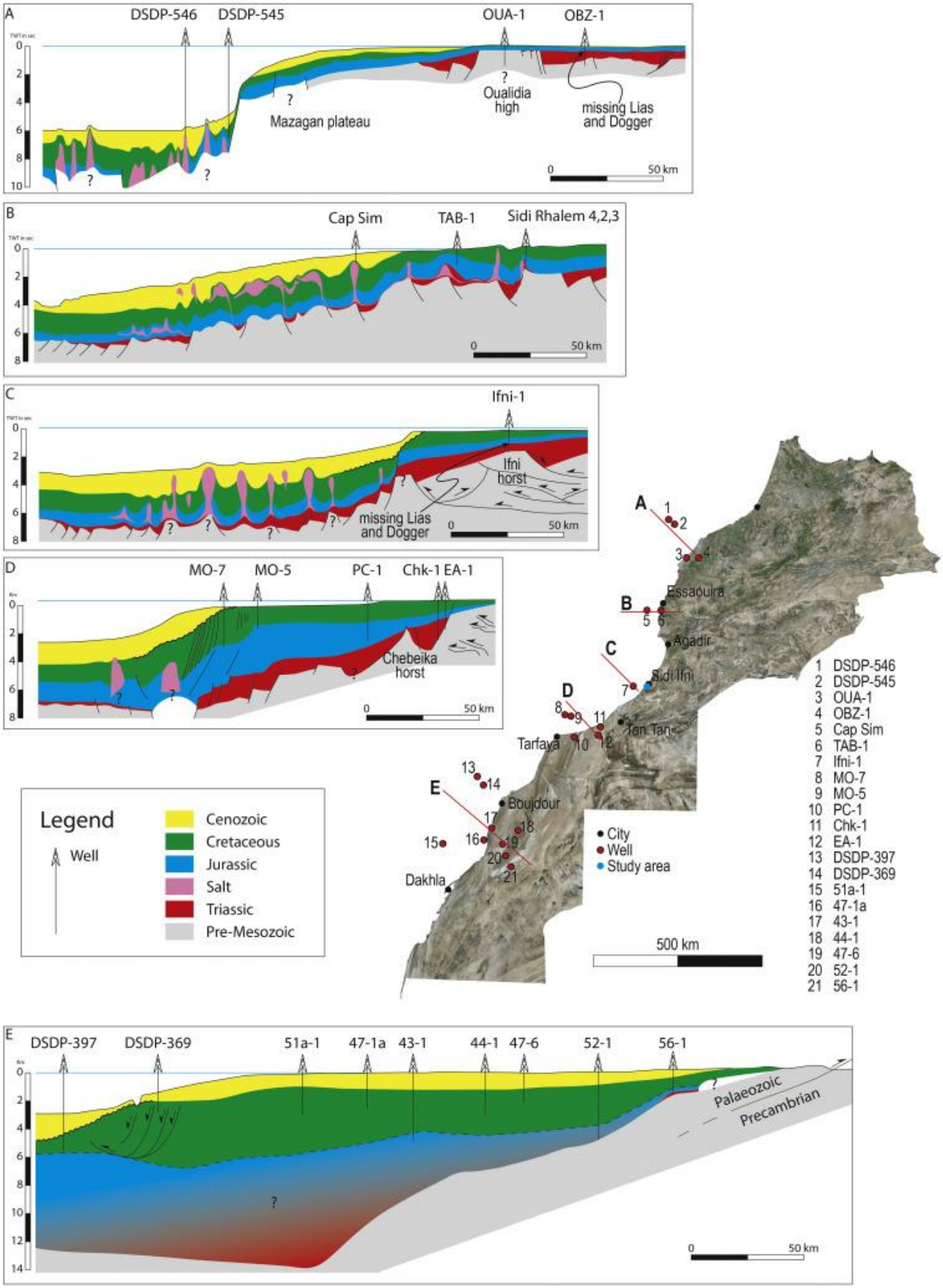
A
DSDP-546
DSDP-545
OUA-1
OBZ-1
Oualidia high
missing Lias and Dogger
Mazagan plateau
0
50 km
B
Cap Sim
TAB-1
Sidi Rhalem 4,2,3
0
50 km
C
Ifni-1
Ifni horst
missing Lias and Dogger
0
50 km
D
MO-7
MO-5
PC-1
Chk-1
EA-1
Chebeika horst
0
50 km
Legend
Well
Cenozoic
Cretaceous
Jurassic
Salt
Triassic
Pre-Mesozoic
Essaouira
Agadir
Sidi Ifni
Tan Tan
Tarfaya
Boujdour
Dakhla
City
Well
Study area
500 km
1 DSDP-546
2 DSDP-545
3 OUA-1
4 OBZ-1
5 Cap Sim
6 TAB-1
7 Ifni-1
8 MO-7
9 MO-5
10 PC-1
11 Chk-1
12 EA-1
13 DSDP-397
14 DSDP-369
15 51a-1
16 47-1a
17 43-1
18 44-1
19 47-6
20 52-1
21 56-1
E
DSDP-397
DSDP-369
51a-1
47-1a
43-1
44-1
47-6
52-1
56-1
Palaeozoic
Precambrian
0
50 km

Fig. 3

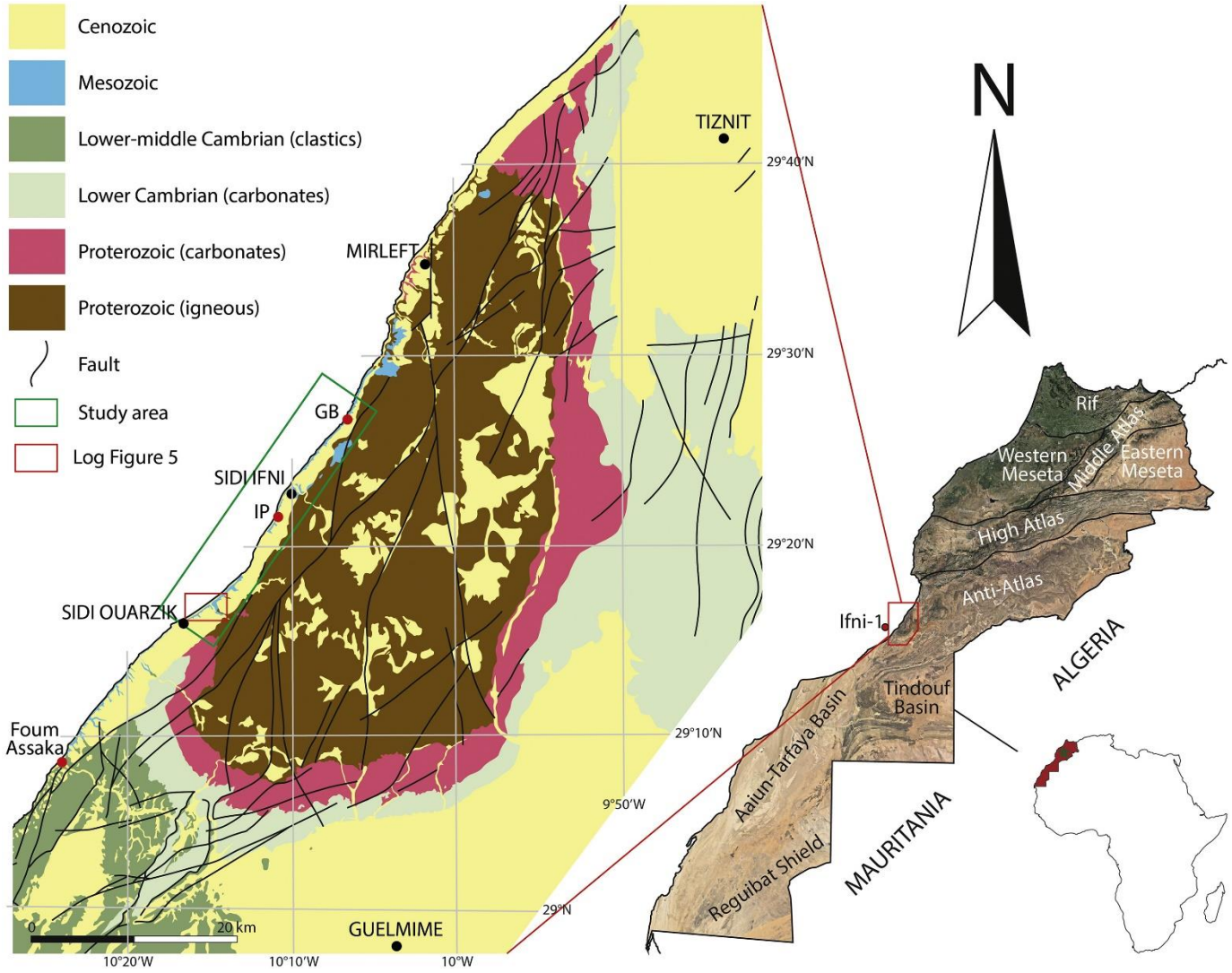
Cenozoic
Mesozoic
Lower-middle Cambrian (clastics)
Lower Cambrian (carbonates)
Proterozoic (carbonates)
Proterozoic (igneous)
Fault
Study area
Log Figure 5
TIZNIT
MIRLEFT
GB
SIDI IFNI
IP
SIDI OUARZIK
Foum Assaka
GUELMIME
29°40'N
29°30'N
29°20'N
29°10'N
29°N
9°50'W
10°20'W
10°10'W
10°W
0
20 km
N
Rif
Western Meseta
Middle Atlas
Eastern Meseta
High Atlas
Anti-Atlas
Ifni-1
Tindouf Basin
Aaiun-Tarfaya Basin
Reguibat Shield
ALGERIA
MAURITANIA

Fig. 4

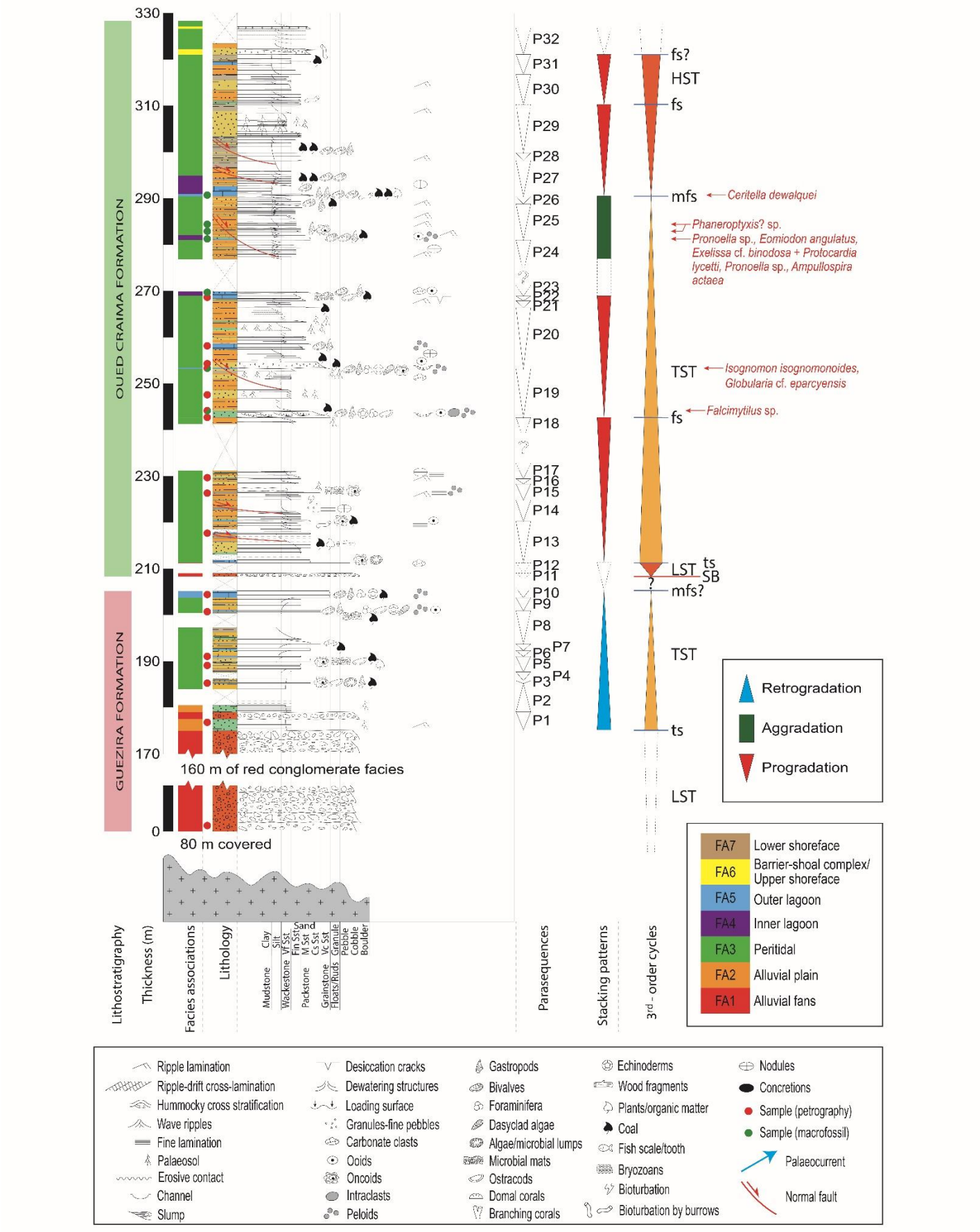
OUED CRAIMA FORMATION
GUEZIRA FORMATION
330
310
290
270
250
230
210
190
170
0
160 m of red conglomerate facies
80 m covered
Lithostratigraphy
Thickness (m)
Facies associations
Lithology
Clay
Silt
Sand
Vf Sst
Fn Sst
M Sst
Cs Sst
Vc Sst
Granule
Pebble
Cobble
Boulder
Mudstone
Wackestone
Packstone
Grainstone
Floats/Ruds
P32
P31
P30
P29
P28
P27
P26
P25
P24
P23
P22
P21
P20
P19
P18
P17
P16
P15
P14
P13
P12
P11
P10
P9
P8
P7
P6
P5
P4
P3
P2
P1
Parasequences
fs?
HST
fs
mfs
Ceritella dewalquei
Phaneroptyxis? sp.
Pronoella sp., Eomiodon angulatus, Exelissa cf. binodosa + Protocardia lycetti, Pronoella sp., Ampullospira actaea
TST
Isognomon isognomonoides, Globularia cf. eparcyensis
fs
Falcimytilus sp.
LST
ts
SB
mfs?
TST
ts
LST
Stacking patterns
3rd - order cycles
Retrogradation
Aggradation
Progradation
FA7 Lower shoreface
FA6 Barrier-shoal complex/ Upper shoreface
FA5 Outer lagoon
FA4 Inner lagoon
FA3 Peritidal
FA2 Alluvial plain
FA1 Alluvial fans
Ripple lamination
Ripple-drift cross-lamination
Hummocky cross stratification
Wave ripples
Fine lamination
Palaeosol
Erosive contact
Channel
Slump
Desiccation cracks
Dewatering structures
Loading surface
Granules-fine pebbles
Carbonate clasts
Ooids
Oncoids
Intraclasts
Peloids
Gastropods
Bivalves
Foraminifera
Dasyclad algae
Algae/microbial lumps
Microbial mats
Ostracods
Domal corals
Branching corals
Echinoderms
Wood fragments
Plants/organic matter
Coal
Fish scale/tooth
Bryozoans
Bioturbation
Bioturbation by burrows
Nodules
Concretions
Sample (petrography)
Sample (macrofossil)
Palaeocurrent
Normal fault

Fig. 5

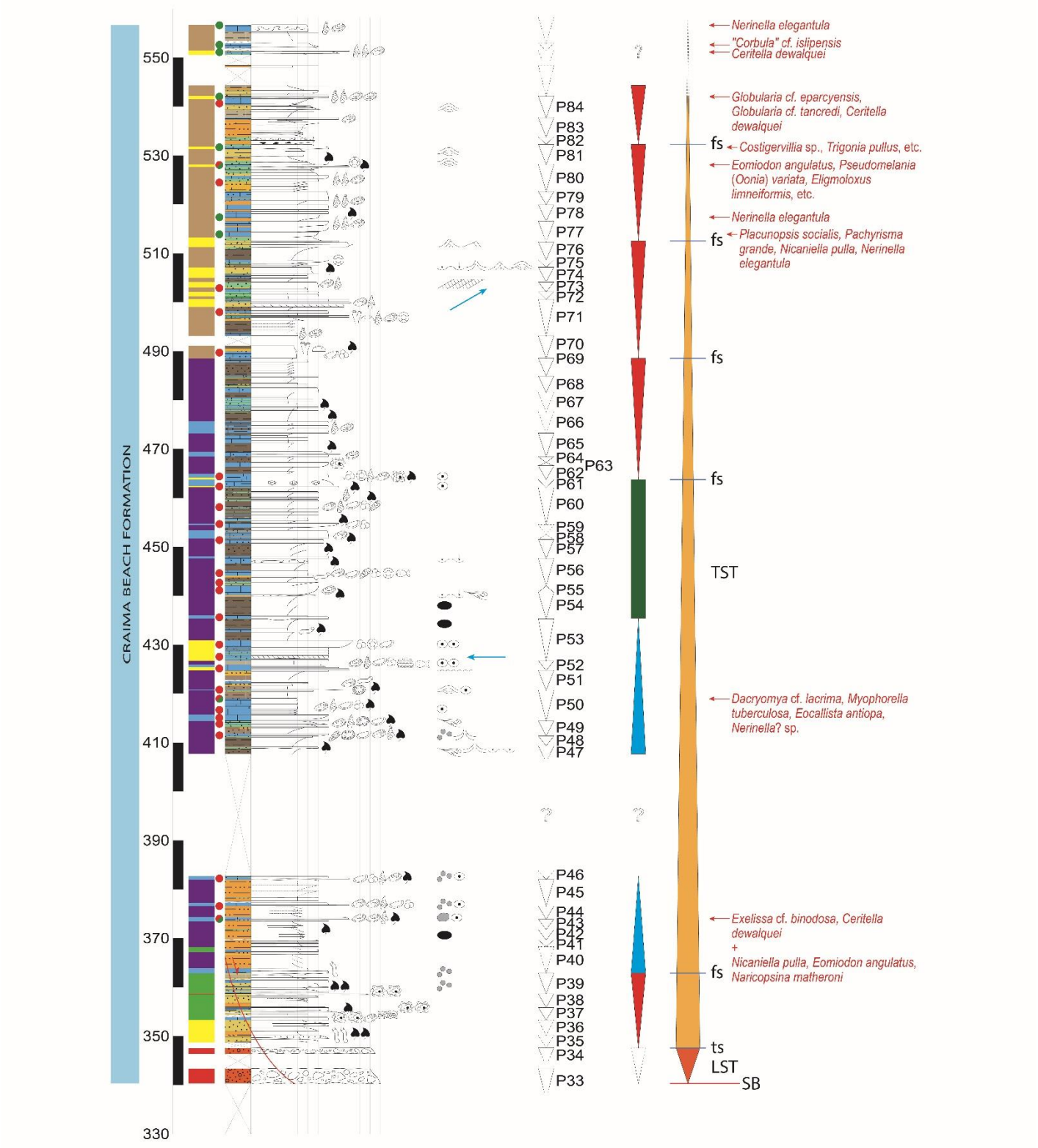
CRAIMA BEACH FORMATION
550
530
510
490
470
450
430
410
390
370
350
330
P84
P83
P82
P81
P80
P79
P78
P77
P76
P75
P74
P73
P72
P71
P70
P69
P68
P67
P66
P65
P64
P63
P62
P61
P60
P59
P58
P57
P56
P55
P54
P53
P52
P51
P50
P49
P48
P47
P46
P45
P44
P43
P42
P41
P40
P39
P38
P37
P36
P35
P34
P33
?
?
?
Nerinella elegantula
"Corbula" cf. islipensis
Ceritella dewalquei
Globularia cf. eparcyensis,
Globularia cf. tancredi, Ceritella
dewalquei
fs
Costigervillia sp., Trigonia pullus, etc.
Eomiodon angulatus, Pseudomelania
(Oonia) variata, Eligmoloxus
limneiformis, etc.
Nerinella elegantula
fs
Placunopsis socialis, Pachyrisma
grande, Nicaniella pulla, Nerinella
elegantula
fs
fs
TST
Dacryomya cf. lacrima, Myophorella
tuberculosa, Eocallista antiopa,
Nerinella? sp.
Exelissa cf. binodosa, Ceritella
dewalquei
+
Nicaniella pulla, Eomiodon angulatus,
Naricopsina matheroni
fs
ts
LST
SB

Fig. 5 (cont.)

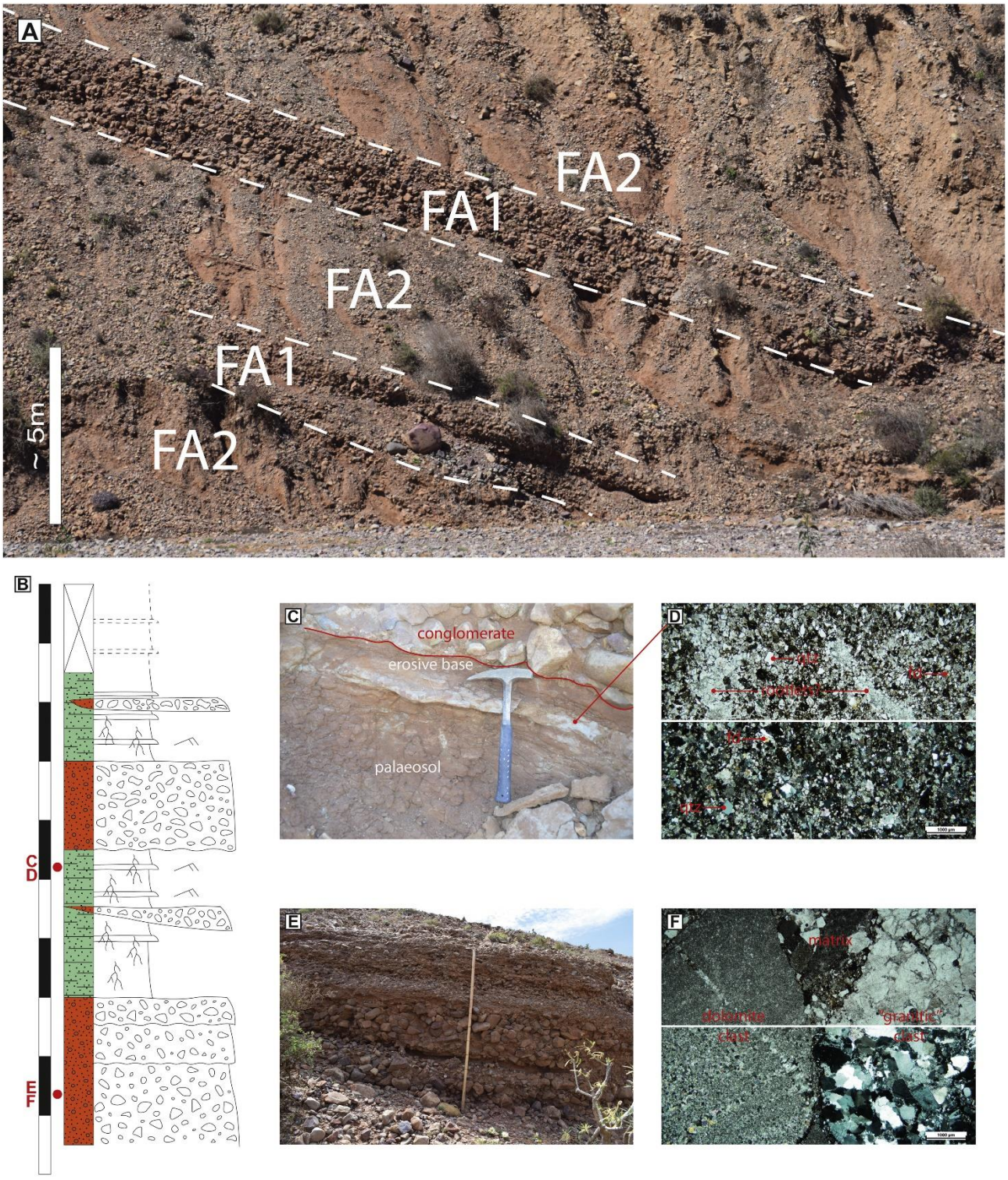
A
FA2
FA1
FA2
FA1
FA2
~ 5m
B
C
D
E
F
conglomerate
erosive base
palaeosol
matrix
dolomite clast
"granitic" clast

Fig. 6

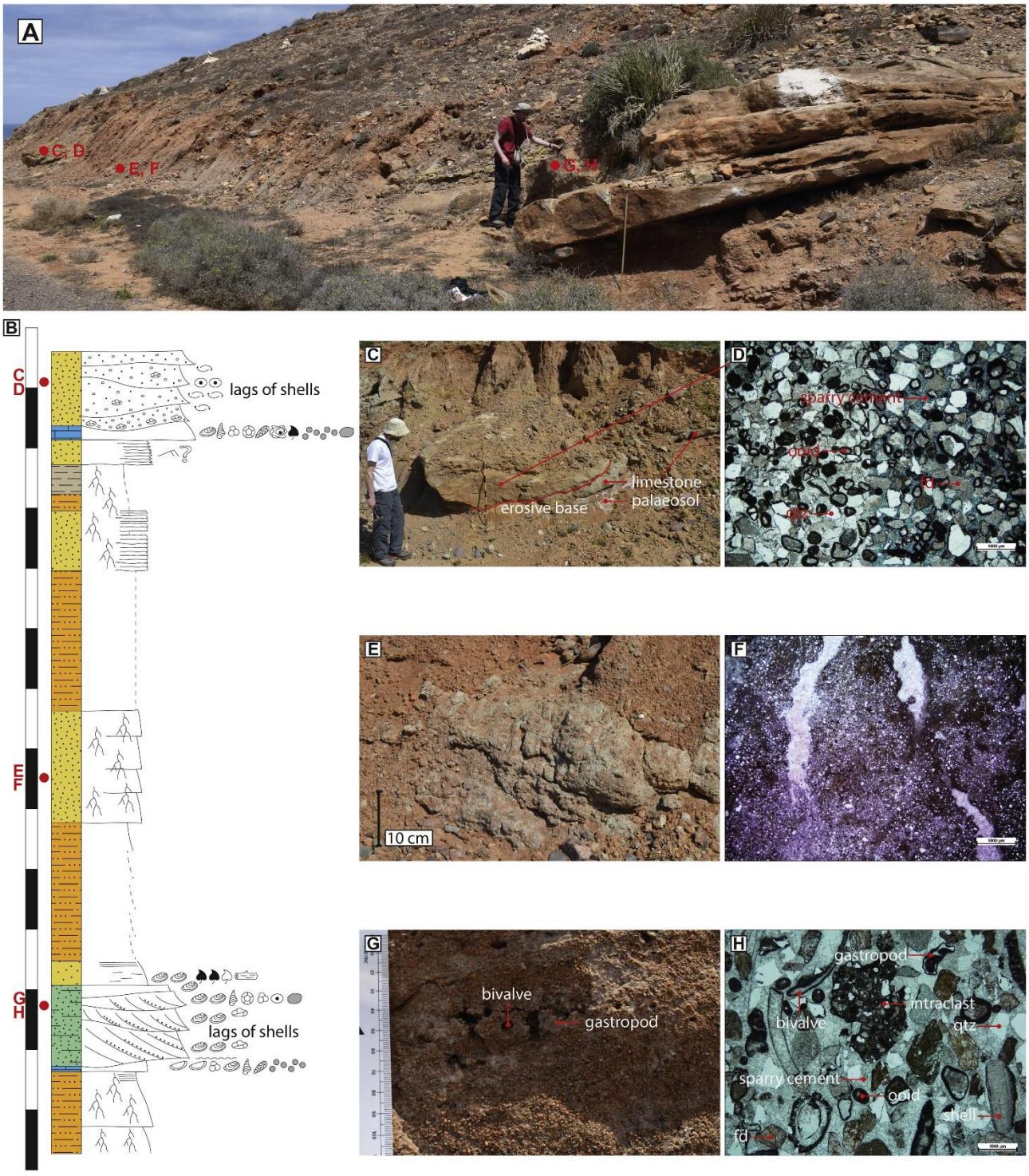
A
C, D
E, F
G, H
B
C
D
lags of shells
limestone
palaeosol
erosive base
sparry cement
ooid
fd
qtz
E
F
10 cm
G
H
bivalve
gastropod
lags of shells
intraclast
shell

Fig. 7

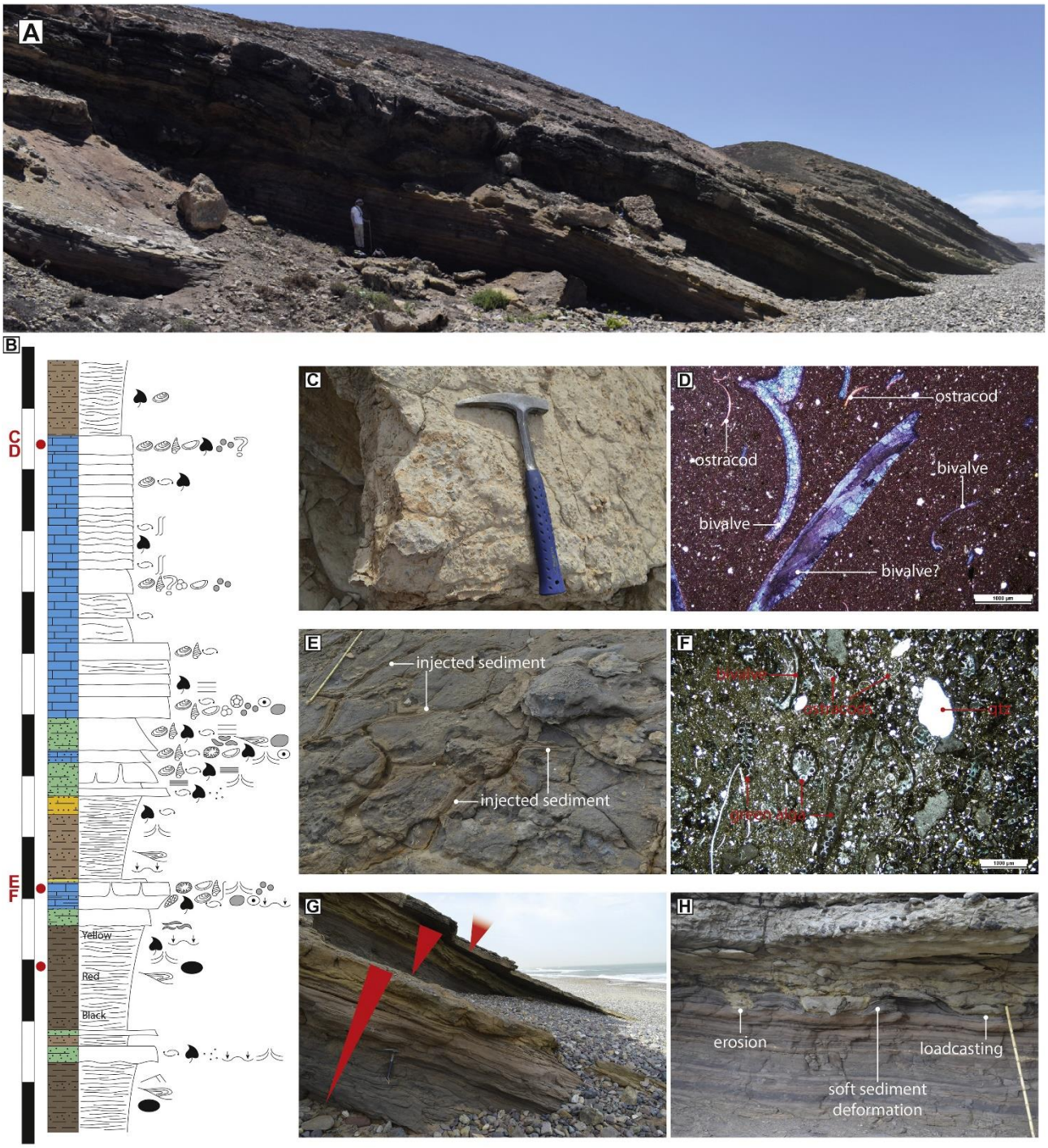
A
B
C
D
ostracod
ostracod
bivalve
bivalve
bivalve?
E
injected sediment
injected sediment
F
bivalve
ostracods
qtz
green algae
G
H
erosion
loadcasting
soft sediment
deformation
C
D
E
F
Yellow
Red
Black

Fig. 8

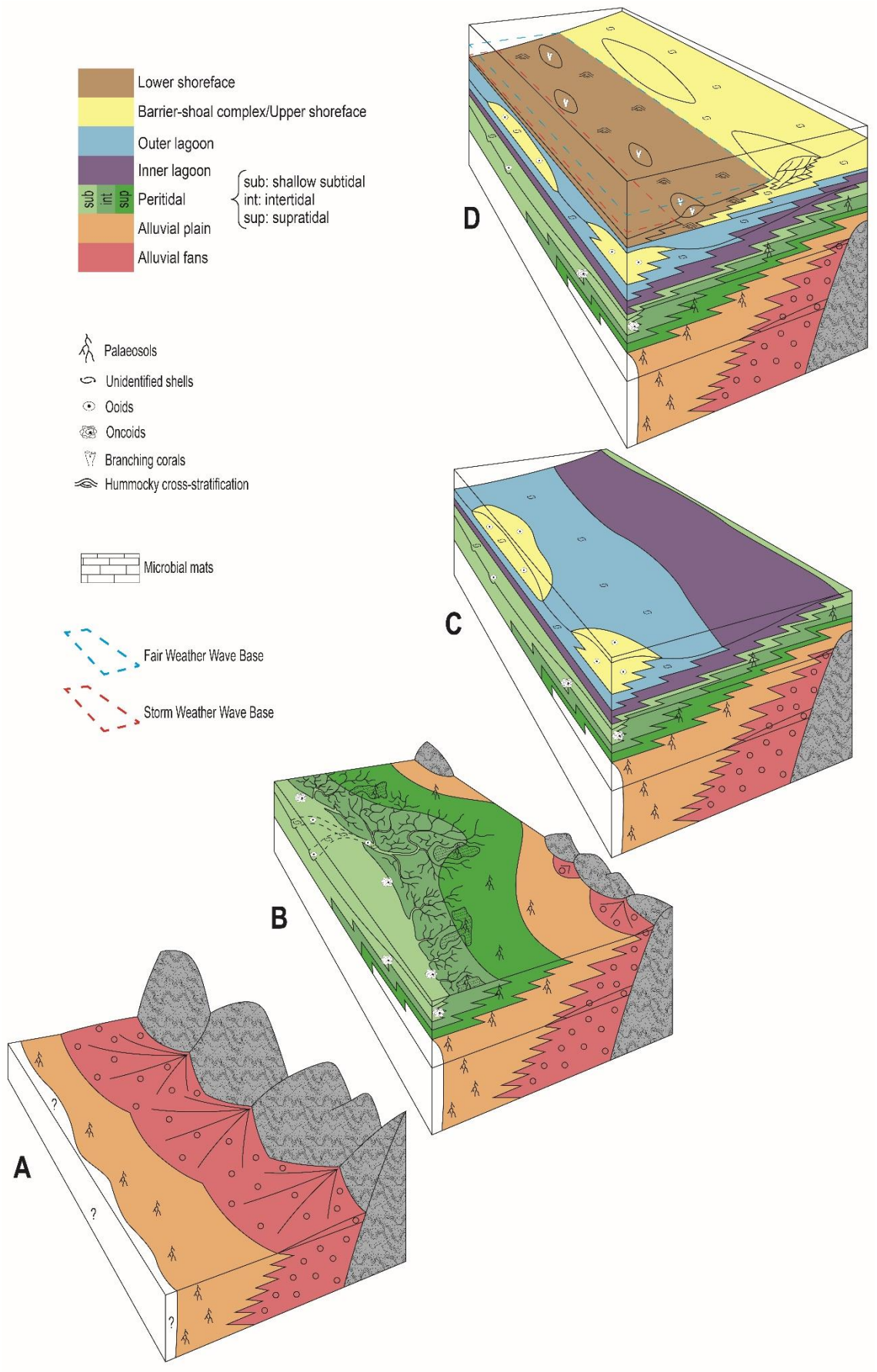
Lower shoreface
Barrier-shoal complex/Upper shoreface
Outer lagoon
Inner lagoon
sub
int
sup
Peritidal
sub: shallow subtidal
int: intertidal
sup: supratidal
Alluvial plain
Alluvial fans
Palaeosols
Unidentified shells
Ooids
Oncoids
Branching corals
Hummocky cross-stratification
Microbial mats
Fair Weather Wave Base
Storm Weather Wave Base
A
B
C
D

Fig. 9

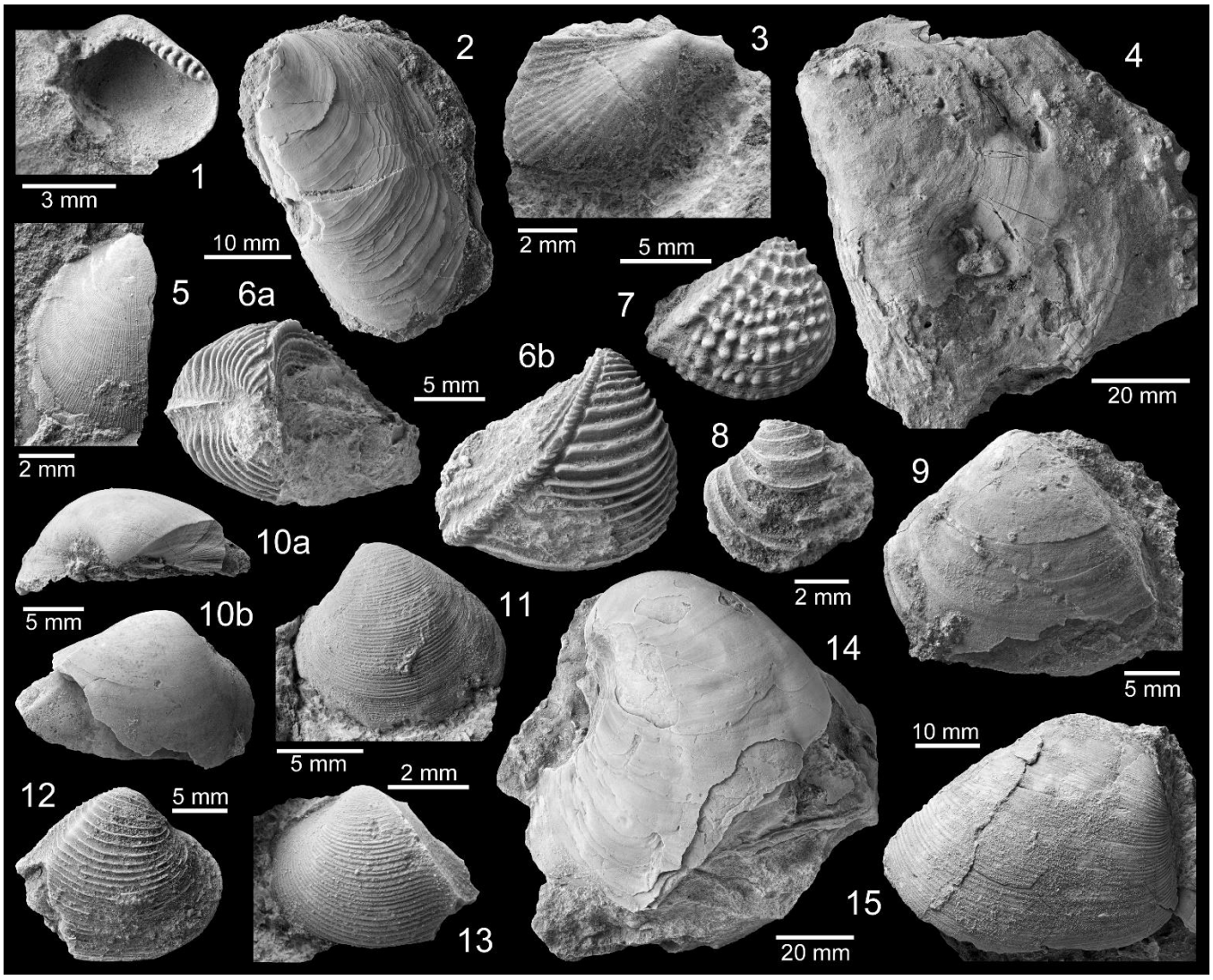
1
3 mm
2
10 mm
3
2 mm
4
20 mm
5
2 mm
6a
6b
5 mm
7
5 mm
8
2 mm
9
5 mm
10a
5 mm
10b
11
5 mm
2 mm
12
5 mm
13
14
15
20 mm
10 mm

Fig. 10

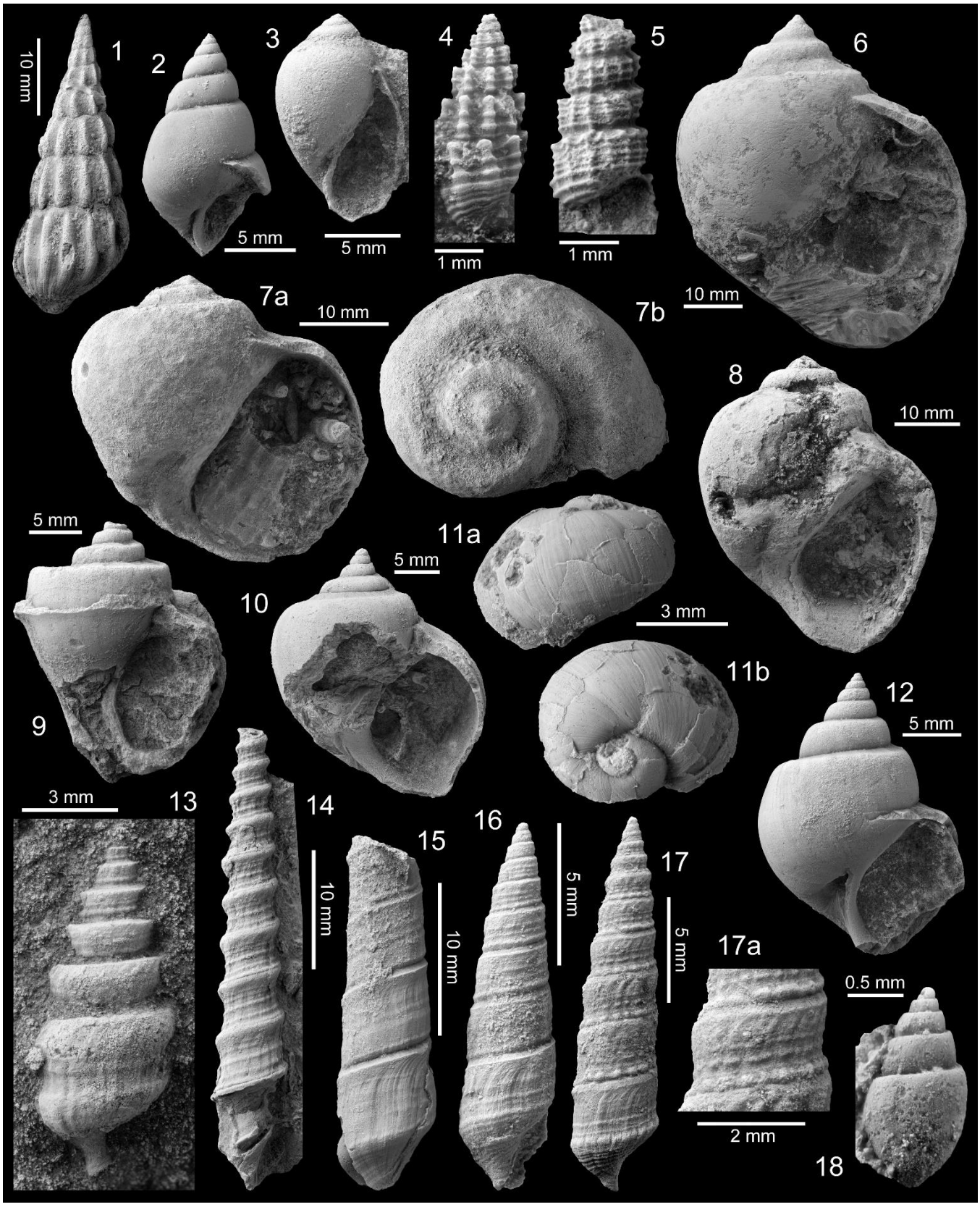
1
10 mm
2
5 mm
3
5 mm
4
1 mm
5
1 mm
6
10 mm
7a
10 mm
7b
8
10 mm
5 mm
9
10
5 mm
11a
3 mm
11b
12
5 mm
3 mm
13
14
10 mm
15
10 mm
16
5 mm
17
5 mm
17a
2 mm
0.5 mm
18

Fig. 11

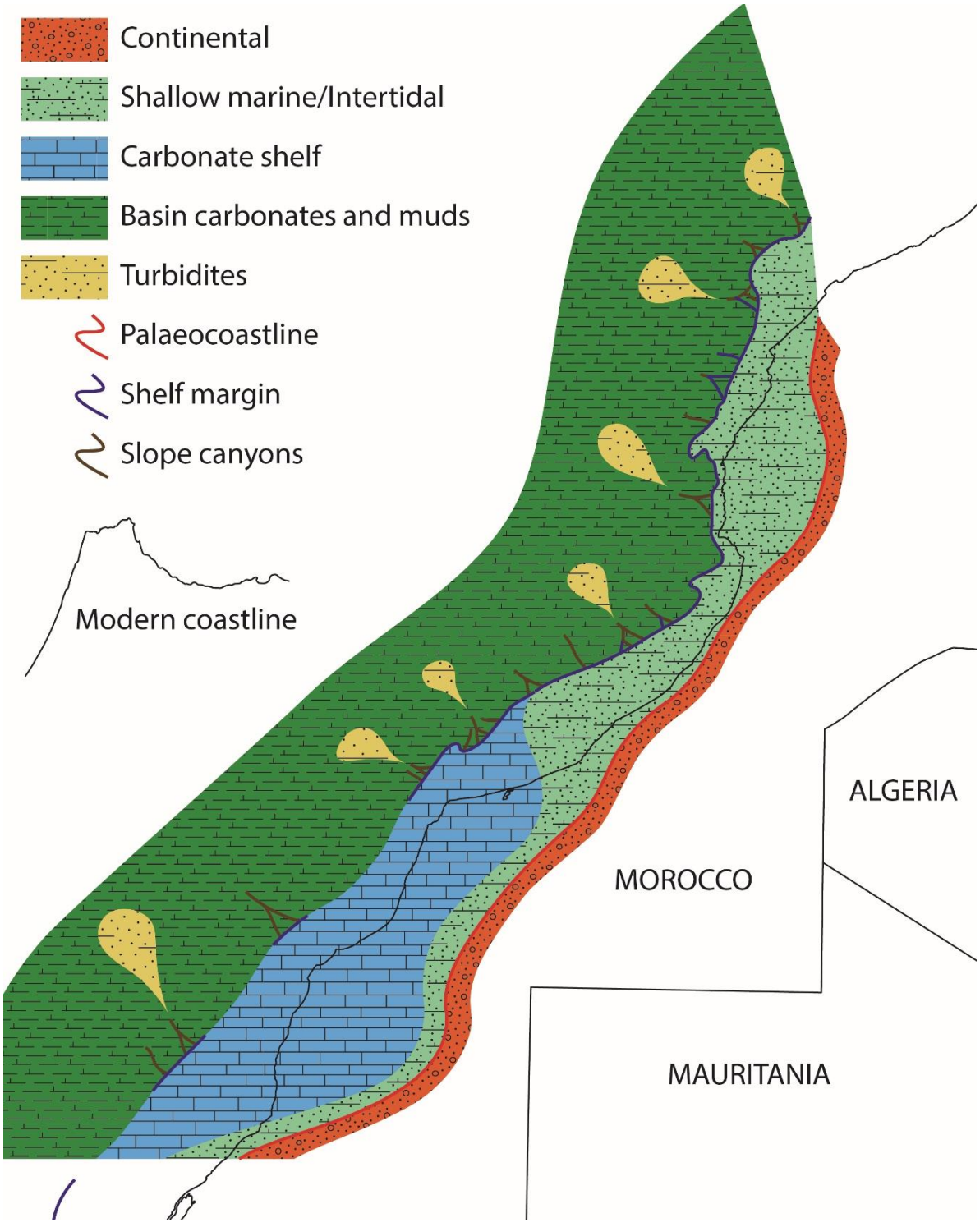
Continental
Shallow marine/Intertidal
Carbonate shelf
Basin carbonates and muds
Turbidites
Palaeocoastline
Shelf margin
Slope canyons
Modern coastline
ALGERIA
MOROCCO
MAURITANIA

Fig. 12

Appendix A. Supplementary data

Table 1. Lithofacies identified at Oued Craima and Sidi Ouarzik successions.

Code	Lithofacies	Description	Interpretation
A	*Normally-graded conglomerates*	Massive to normally graded clast-supported red conglomerates. Beds are 10 to 70 cm thick laterally continuous with erosive base, rarely channelised (up to 20 m wide) and lacking clast imbrication or cross-bedding. Clasts have heterogeneous composition (sedimentary, igneous and metamorphic) and size ranges from 2 mm to 60 cm (from angular to rounded depending on the location).	Migration of broad bars and dunes in unconfined gravel sheets
B	*Inversely graded conglomerates*	Inversely-graded, sometimes matrix-supported, red conglomerates. Beds are 10 to 50 cm thick, laterally discontinuous (up to 10-15 m) with erosional basal surfaces or draping previous topography. Clast composition is heterogeneous (sedimentary, igneous and metamorphic), subangular to rounded with a maximum grain size up to 15 cm.	Pseudoplastic debris flow in unconfined gravel sheets
C	*Matrix-supported granule-pebble conglomerate*	Structureless (to slightly normally graded) wavy to irregularly bedded matrix-supported brownish-grey pebble conglomerate. Top of individual beds can be wave- (and current-) rippled. Beds range from a few cm to 15 cm thick with sharp contacts and sometimes with pebbles accumulated in scoured bases. Occasional cm thick interbeds of muds. Floating granules and cm-scale pebbles are rounded to subrounded and pebbles may be absent. Matrix grain size ranges from fine-grained to very coarse-grained. Common bioturbation by vertical burrows (possible *Diplocraterion habichi*, *Arenicolites* or *Skolithos*) up to 20 cm long.	Ripples and scattered pebble-size clasts indicate high energy oscillatory and unidirectional currents. Interbedded thin muds suggest periods dominated by suspension settling. Long vertical bioturbation suggests high sedimentation rates.

D	*Crossbedded fine- to very coarse-grained sandstones*	Fine- to very coarse-grained normally graded cross- and parallel-bedded sandstone. Beds up to 60 cm thick with cross sets 20-40 cm-thick, erosive sharp base or loadcasted. Granules and pebbles up to 2 cm can be common either scattered, forming lags along foresets or even present towards the top of some beds together with scattered shell fragments. Sedimentary structures can also include current and wave ripples on the tops of some beds and possible herring-bone cross-stratification. Bioturbation and accumulation of bivalves and gastropods can be important at the base of some beds.	Migration of dunes under uniderectional flow puctuated by wave reworking. Rare storm- and bidirectional current-reworking.
E	*Ripple-laminated sandstone*	Fine-grained ripple cross-laminated sandstone with possible interlamination of silts. Beds are cm thick and the most striking sedimentary structures are climbing ripples. Clasts are mainly quartz, feldspar and opaques from subrounded to subangular.	Unidirectional current migration of ripples under conditions of high sediment supply
F	*Very fine- to medium-grained calcareous sandstone to packstone*	Yellow to withish very fine- to medium-grained calcareous sandstone with variable silt content. Structureless irregular, tabular to undulating cm thick beds up to 30 cm thick with sharp to gradual contacts commonly dewatered or loadcasted and locally erosive. Internally it may have basal parallel bedding, sometimes slumped or contorted internal bedding. Occasionally, beds are inverselly graded (bioclast content increase upwards). Rare ripple cross lamination. Clastics include subrounded to angular quartz, feldspar, rock fragments and dolomite clasts in variable proportions. Bivalves, gastropods and ostracods can be from absent to abundant, including cm-scale gastropods. Other components include rip-up mud clasts, irregular ooids, scattered granules and pebbles, carbonaceous plant fragments and carbonate clasts (up to 15 cm). Rare wood fragments, galuconite, intraclasts and algal mat fragments. Usually rich in micritic matrix. Occassionally, bioturbation by *Thalassinoides* can be pervasive at the base of individual beds.	Dewatering structures and slumps suggest rapid deposition in a relatively steep marine environment. High content in subspheric and subrounded clastics, broken and abraded bioclasts and relatively small size of alloctonous microbial clots suggest agitated environment. Most of the

			bioclasts are probably alloctonous
G	*Massive sandstone*	Massive very fine to fine-grained red sandstone. Bed thickness ranges from a few cm to 25 cm. Lack of sedimentary or biogenic structures may be due to poor exposure and weathering.	Despite the lack of diagnostic structures association with surrounding lithofacies suggests overbank unconfined pulsatory (or wanning) flows.
H	*Normaly graded calcareous sandstone and silts*	Very fine-grained white calcareous wavy-, parallel- or ripple cross-laminated sandstones with rootlets grading into very fine-grained clay- to silt-rich red sandstones. Bed thickness ranges from 10 to 50 cm with sharp base (not erosive) and top. White basal sandstones are 5-10 cm thick. Main clasts are quartz, detrital dolomite, and feldspars, calcite-cemented and patches rich in iron oxides. Sedimentary structures include wavy-, parallel- and ripple cross-lamination in the lower white part and wavy to discontinuous thin bedding to lamination in the upper red ("chippy" texture) with extremely rare cross-lamination and sparse rootlets.	Lamination and ripples suggest lower flow regime conditions of unidirectional unconfined wanning flows. Rootlets and precipitation of calcite and oxides indicate soil formation

I	*Wavy- to hummocky cross-laminated (bedded) sandstones*	Laminated / bedded to hummocky cross-stratified very fine- to coarse-grained, sometimes calcareous, sandstones and interlaminated muds. Beds are 15-50 cm thick with wavy contacts. Additional sedimentary structures include occasional planar cross-bedded sets up to 15 cm thick and wave ripples. Main clasts are quartz and feldspar. Gastropods, bivalves and scarce echinoderms may be present.	HCS generated by storm waves below the fair weather wave base combined with bars formed under unidirectional flows (planar cross-bedding) and wave reworking.
J	*Mottled to laminated palaeosols*	Massive to laminated micrite-rich and carbonate-cemented clay to fine-grained sandstones, usually mottled or with "chippy" texture in outcrop. Thickness ranges from a few cm up to 1.5 m. Contacts are diffuse to sharp and very irregular. Internal sedimentary structures are usually absent but occasional ripple cross-lamination is possible, but unfrequent. A wide range of detrital clasts includes angular to subrounded quartz, feldspars and opaques, minor reworked microbial lumps, peloids, intraclasts, filosilicates, microcodium fragments and heavy minerals, and traces of ostracods and unidentified bioclast fragments.	Absence of sedimentary structures is probably due to intense bioturbation and cementation processes. Ripples suggest traction in unconfined flows. Micrite has mixed origin from suspension settling and chemical precipitation related with exposure and carbonate soil formation. Occasional restricted marine fauna is interpreted as occasional marine connection through bidirectional flows.

K	*Reworked mud to sandstone and carbonate clasts bed.*	Bed 35 cm thick made of mud, silt, sand and carbonate clasts up to 6 cm in size. Usually clast-supported but clasts can be also floating in a sitly-sandy matrix. No apparent internal structure. Frequently irregular to wavy sharp erosional base and sometiems gradational top.	Plastic debris flow
L	*Clayey siltstones to very fine-grained sandstones*	Normally graded to massive yellow, red to grey clayey siltstones to very fine-grained sandstones with occasional cm thick interbeds of medium-grained sandstone. Bed thickness ranges from 5 cm to 1 m thick with flat to undulating basal and upper contacts, sometimes diffuse or interfingered with underlying and overlying beds. Internal irregular lamination may be present likely due to subtle changes in grain size. Occasional intense bioturbation may destroy any previous internal structure (massive appearance). Ripples may be relatively abundant in some parts of the succession usually related with the coarser spectrum of the grain size. Carbonaceous plant fragments and plant fragments are relatively abundant and sparse wood fragments. Fossils are rare but when present they can be very abundant and monospecific (cm-scale, thin-shelled *Falcimytilus* sp.). Frequent carbonate nodules following the bedding. Nodules can coalesce laterally and form continuous beds. Unidentified burrowing disturbing lamination can be intense but not common. Scarce horizontal burrows and possible rootlets.	Normal grading and ripples generated under lower flow regime conditions in unconfined wanning unidirectional flows combined with suspension settling. Abundant monospecific thin-shelled bivalves and / or intense bioturbation is interpreted as a quiet subaquatic setting with certain degree of stress.

M	*Laminated to thinly bedded dark clays to very fine-grained sandstones*	Alternating wavy laminated to thinly bedded black clays to red-yellow silts and very fine-grained sandstones. Thickness ranges from mm to cm scale. Erosional surfaces, small-scale slumps and dewatering structures can be locally abundant. Sub-milimeter carbonaceous plant fragments are very abundant together with sparse wood fragments. Bivalves and bioturbation are extremely rare.	Grain size variation, erosive surfaces, dewatering structures, absence of fauna and bioturbation together with abundance of carbonaceous plant fragments represent rapid deposition under unconfined fluctuating hyperpycnal flows with possible periodic suspension settling between events. Slumping suggest a steep setting.
N	*Algal laminated quartz-bearing packstone*	Interlaminated peloidal boundstones, microbial / algal stromatolite-like mats, peloidal packstones to wackestones. Beds range in thickness between 5 to 20 cm with wavy contacts and occasionally can look slightly nodular. Dessication cracks are rare and only identified in thin section. Lamination at microscopic scale is determined by alternation of quartz- or reworked peloid-rich packstone (to wackestone) lamina with biologically induced / bound carbonates. Main components include clots of biologically-trapped silt-sized subspherical peloids and scattered fragments of reworked microbial / algal mats up to 2.5 mm in size. Resedimented peloids can be locally predominant, together with variable proportions of silt-sized angular to subangular clastic quartz, feldspars, rock fragments and opaques, scattered	Alternation of lamina of reworked material with biologically induced carbonates suggests traction by unconfined pulsating flows and periods of no deposition with exposure (dessication cracks). Fauna assamblages indicate

		medium- to coarse-grained sand-sized subangular quartz, rock fragments and feldspars, ostracods, gastropods and bivalve bioclasts and scattered spherical to subspherical sand-sized multicoated radial ooids. Micritic matrix is not homogeneously distributed and may alternate with lamina richer in sparry cement filling fenestral porosities.	connection with moderately restricted marine environments probably transported by bidirectional flows. Micrite probably has two origins, from suspension settling and chemically precipitated during initial soil formation.
O	*Bioclastic-oolitic quartz-bearing grainstone (locally packstone)*	Normally graded coarse-grained to granule-sized, sometimes crossbedded and channelised, grainstone. Channel thickness can be up to 1.2 m and cross bedded sets up to 15 cm. Additional sedimentary structures may include lags of granules and shell fragments. Components include variable proportions of bivalve and gastropod broken fragments up to 4 mm-long commonly displayed subparallel to bedding, microbial / algal fragments and intraclasts of a wide range of compositions and sizes (up to mm-scale), common sand-sized ooids, rock fragments of a wide range of compositions, sphericity and roundness up to 2.5 mm, and silt- to coarse sand-sized quartz and feldspars, minor oolitic packstone / grainstone (up to 2.5 mm) and micrite intraclasts, echinoderm fragments, agglutinated benthic foraminifera (*Reophax* sp. probably), ostracods, phyllosilicates and other sedimentary minerals. Micritic matrix is mostly absent but can be present in layers parallel to bedding.	Channelised bases, crossbedding and broken bioclasts indicate high energy traction of confined flows. Alternation of a mixture of open and restricted marine fauna and continent-derived components, together with grainstone and packstone textures suggest tide-related bidirectional flows.

P	*Oncoid-bearing packstone*	Light grey oncoid-bearing (silty) packstone (occasionally wackestone). Wavy to planar beds 10 to 50 cm thick with sharp base and top. Main components include variable proportions of mm-scale oncoids, peloids, carbonaceous plant fragments, ostracods, microbial / algal lumps and intraclasts. Oncoids are mainly either porostromate-like with fenestral fabric or spongiostromate. Silt-sized terrigenous subangular quartz and feldspars can be relativelly abundant together with subordinated igneous and metamorphic rock fragments and detrital phyllosilicates. Usually, minor gastropods, bivalves, benthic foraminifera and ooids and traces of wood and echinoderm fragments and possible bryozoans.	Oncoids are typical in shallow subtidal to lower intertidal settings with moderate agitation. Fossil assamblages suggest moderately stressed marine environment with more or less connection with normal conditions. Relative abundance of terrigenous clasts is related with proximity to the continent.
Q	*Calcareous siltstones-sandstones to silty packstones*	Massive to chaotic light grey siltstones to fine-grained sandstones. Bed thickness ranges from 5 to 15 cm, sharp irregular to erosive base and sharp top. Lithologies can range from clastic- to carbonate-dominated. Carbonaceous plant fragments are abundant. Occasionally, broken bivalves and gastropods are abundant. Reworked carbonate clasts up to 10 cm in size are possible.	Erosive bases and reworked clasts from continental and marine origin suggest high energy.
R	*Mudstone (to wackestone)*	Massive to thinly bedded light to dark grey micritic mudstones. Wavy to irregular beds, almost nodular sometimes, 5-30 cm thick, sometimes affected by soft sedimentary deformation. Bioclast-poor beds are usually intensely bioturbated at the base (*Thalassinoides* and possible *Planolites*). Components include different amounts of disarticulated bivalves, gastropods (up to several cm), silt-sized quartz clasts, carbonaceous plant fragments, ostracods, peloids, benthic foraminifera, dasycladaceas and ooids.	Mainly suspension settling and autochthonous fauna. Fine grained carbonate mud and absence of sedimentary structures is interpreted as

			indication of quiet and relatively deep conditions.
S	*Bioclast-bearing silty peloidal wackestone to packstone*	Massive to irregularly bedded grey bioclastic-bearing peloidal wackestone to packstone. Tabular bedding 5-40 cm thick with irregular to wavy sharp contacts, nodular and almost discontinuous sometimes, occasionally load casted and dewatered. Rare large-scale soft-sediment deformation and local erosive bases. Rare "lags of floating" bivalves and cm-scale gastropods. Grains include silt-sized peloids, intraclasts and quartz clasts, relatively abundant bivalves (sometimes thin-shelled), gastropods (nerinellids) and carbonaceous plant fragments. Dasycladacean (*Holosporella siamensis*) and lumps of unidentified blue - green algae up to 2 mm in size can be locally the main allochem. Scattered intraclasts, ooids, wood fragments, scattered granules and pebbles; and reworked carbonate clasts up to 7 cm in size may or may not be present. Scattered cm-scale gastropods may be present on top of individual carbonate beds. Ostracods may keep both valves preserved. Benthic foraminifera (agglutinated, textularids and miliolids among others), wood fragments, fish remains, regular echinoderms and silt-sized quartz and feldspar.	Combined episodes of rapid sedimentation (soft-sediment deformation and erosion) under moderate to high energy conditions and suspension settling. Fauna assemblage suggests shallow moderately restricted conditions with some open marine influence.
T	*Peloidal packstone*	Massive to faintly irregularly laminated peloidal packstones. Irregular to wavy bedding 10-15 cm thick. Sand-sized ovoid elongated to irregular peloids are the main allochem. Other grains include silt-sized quartz, ostracods, ooids, gastropods, bivalves, benthic foraminifera, carbonaceous plant fragments, microbial mats fragments and echinoderm fragments may or may not be present.	Lack of sedimentary strutures suggests micritic mud settled from suspension together with accumulation of autochthonous fauna.

			Admixtures of continent-derived clastics and bio-laminites and normal marine conditions bioclasts suggest weak currents and agitation.
U	*Silty (sandy) grainstone with blue / green algae*	Irregularly bedded silty / sandy grainstone to packstone with algae. Bed is 20 cm thick with irregular sharp surfaces, cross-bedding, shell lags and mud drapes (micritic)? Main allochems are sand-sized quartz, feldspar and rock fragments, intraclasts up to 3 mm and blue - green algae fragments up to several mm in size. Minor opaques, carbonaceous plant fragments. Scarce full and broken radial ooids. Bivalves in outcrop.	Sedimentary structures suggest traction and rapid deposition under energetic pulsating flows alternating with suspension settling.
V	*Peloidal- and bioclastic-bearing grainstone*	Massive to laminated peloidal and bioclastic-bearing grainstones. Beds are tabular, 5-30 cm thick with irregular to wavy contacts, occasionally loadcasted. Occasionally bioclast content increases slightly towards the top of individual beds. Main allochems include variable proportions of broken bivalves and gastropods, subspherical peloids silt- to fine sand-graded (possible fecal pellets), benthic foraminifera (agglutinated, miliolids and textulariids mainly). Aggregates, intraclasts and composite ooids can be from common to traces. Subordinate components are wood and carbonaceous plant fragments, micrite concentric ooids (scarce with radial fabric), and broken echinoderm plates and spines. Minor dasyclads. None to very little silt-sized subangular to subrounded quartz and feldspar clasts. Possible bryozoans are extremely rare. Micritization rims can be thick and peloids are frequently allochem completely micritised.	Fauna assemblages are typical of normal to moderately restricted marine conditions. Broken bioclasts and absence of micrite suggest an agitated environment. Common micrite envelopes relates with deposition in a shallow marine setting.

W	*Oolitic grainstone*	Massive to normally graded grey oolitic grainstones. Beds are 15-25 cm thick with very sharp irregular erosive bases and occasionally loaded. Faint internal thin bedding (perhaps cross-bedding). Main grains are spherical to ovoid sand-sized concentric micritic ooids, silt- to sand-sized spherical to ovoid peloids and intraclasts up to 3 mm in size. Minor broken bivalves and gastropods, disarticulated ostracods and aggregates. Traces of benthic foraminifera, briozoa and likely fish scales. Possible microkarst developed on some beds. Rare bioturbation by *Thalassinoides*, but may be intense locally.	Abuntant ooids and sedimentary structures indicate shallow energetic waters with possible short-timed exposure (possible microkarst)
X	*Cross-bedded sandy grainstone (packstone)*	Normally graded cross-bedded quartz- and feldspar-rich oolitic grainstone. Beds are 15-60 cm thick with sigmoidal to tangential cross-bedding and sharp erosive bases. Foreset surfaces may be reworked subperpendicularly by waves (wavy ripples). Possible mud drapes on foresets. The majority of grains are sand-sized K-feldspar and quartz, many of them coated by one layer of micrite (incipient ooids) and far less abundant silt- to very fine sand-sized subspherical peloids. Minor subspherical sand-sized radial ooids cored by incipient ooids (first micritic layer). Traces of carbonaceous plant fragments, ostracods, gastropod and bivalve fragments. Minor ostracods and pebble-sized quartz up to 2 cm can be present. Occasional bioturbation. Micritization can be intense destroying the primary texture of some grains.	Migration of dunes under unidirectional currents modulated by wave reworking
Y	*Coral-rich packstone*	Massive, chaotic to faintly laminated, undulating coral-bearing packstone. Beds are 10-50 cm thick and bases can be erosive and loadcasted. Usually, scattered coral fragments are present but individual beds can be packed with broken fragments of branching corals and minor bulbous corals. Additional grains include silt-sized quartz and feldspar (some fd up to 400 microns), peloids, bivalves and gastropods up to several mm in size. Minor ostracods, intraclast / microbial clot fragments, echinoderm fragments and carbonaceous plant fragments.	Fragmented bioclasts and sedimentary structures suggest rapid deposition in high energy waters. Branching coral usually develop in quiet water within the photic zone.

Table 2. Additional information about stratigraphic range and geographical distribution of bivalves from Oued Craima and Sidi Ouarzik.

BIVALVIA

Species	Stratigraphic range	Geographic distribution	References
***Dacryomya* cf. *lacrima* (J. de C. Sowerby, 1824)**	Bathonian-Lower Callovian	northern Germany, England, India	Stoll (1934); Cox and Arkell (1948); Jaitly et al. (1995)
***Isognomon isognomonoides* (Stahl, 1824)**	Aalenian-Bajocian	England, Paris Basin	Benecke (1905); Cox and Arkell (1948)
	Bajocian	Romania	Lazăr (2006)
	Bathonian	England, Paris Basin	Cox and Arkell (1948); Fischer (1969); Palmer (1979)
***Placunopsis socialis* Morris & Lycett, 1853**	Bathonian	Paris Basin, England	Cossmann (1907); Cox and Arkell (1948); Fischer (1969); Palmer (1979); Todd and Palmer (2002)
***Trigonia pullus* J. de C. Sowerby, 1826**	Bathonian	Egypt, England, Paris Basin, Tunisia	Douvillé (1916); Cox and Arkell (1948); Fischer (1969); Holzapfel (1998); Palmer (1979)
***Myophorella tuberculosa* (Lycett, 1850)**	Aalenian?-Bajocian	England	Lycett (1850)
	Bathonian	Paris Basin	Fischer (1969)
***Nicaniella pulla* (Roemer, 1836)**	Uppermost Bajocian-Upper Bathonian	Poland	Pugaczewska (1986)
	Lower Bathonian-Middle Callovian	northern Germany	Stoll (1934)
***Protocardia lycetti* (Rollier, 1912)**	Bathonian	Paris Basin, England	Cossmann (1900); Cox and Arkell (1948); Palmer (1979)
***Eocallista antiopa* (d'Orbigny, 1850)**	Bathonian	England, Paris Basin	Cox and Arkell (1948); Fischer (1969); Palmer (1979)

***Eomiodon angulatus* (Morris & Lycett, 1855)**	Bathonian	England, southern France, China?	Cox and Arkell (1948); Yin and Fürsich (1991); Fürsich et al. (1995)
***"Corbula"* cf. *involuta* Münster in Goldfuss, 1837**	Bajocian?	southern Germany	Goldfuss (1837)
	Bathonian	England, southern France	Lycett (1863); Cossmann (1905)
***"Corbula"* cf. *islipensis* Lycett, 1863**	Bathonian	England, Paris Basin	Lycett (1863); Fischer (1969)
***Pachyrisma grande* Morris & Lycett, 1850**	Bathonian	England	Cox and Arkell (1948)
***Ceratomya concentrica* (J. de C. Sowerby, 1825)**	Bajocian-Oxfordian	Europe, Africa, Middle East	de Loriol (1883); Douvillé (1916); Cox (1936, 1965); Cox and Arkell (1948); Fischer (1969)

References

Benecke, E.W., 1905. Die Versteinerungen der Eisenerzformation von Deutsch-Lothringen und Luxemburg. Abhandlungen zur geologischen Spezialkarte Von Elsass-Lothringen, N.F. 6, 1–598.

Cossmann, M., 1900. Seconde note sur les Mollusques du Bathonien de Saint-Gaultier (Indre). Bulletin de la Société Géologique de France 3ème série 28, 165–203.

Cossmann, M., 1905. Sur un gisement de fossiles bathoniens près de Courmes (Alpes-Maritimes). Bulletin de la Société Géologique de France. 4ème série 2, 829–846.

Cossmann, M., 1907. Troisième note sur le Bathonien de Saint-Gaultier (Indre). Bulletin de la Société Géologique de France 4ème série 7, 224–253.

Cox, L.R., 1936. Fossil Mollusca from southern Persia (Iran) and Bahrein Island. Memoirs of the Geological Survey of India, Palaeontologia Indica, new Ser. 22 (2), 1–69.

Cox, L.R., 1965. Jurassic Bivalvia and Gastropoda from Tanganyika and Kenya. Bulletin of the British Museum (Natural History) Geol. Suppl. 1, 1–213.

Cox, L.R., Arkell, W.J., 1948. A survey of the Mollusca of the British Great Oolite Series, primarily a nomenclatorial revision of the monograph by Morris & Lycett (1851–55), Lycett (1863), and Blake (1905–1907). Part 1. Monograph of the Palaeontographical Society of London 102, 1–48.

de Loriol, P., 1883. Étude paléontologique et stratigraphique des Couches à Mytilus des Alpes vaudoises. Mémoires de la Société Paléontologique Suisse 10, 1–95.

Douvillé, H., 1916. Les terrains secondaires dans le massif du Moghara à l'est de l'isthme de Suez d'après les explorations de M. Couyat-Barthouse. Paléontologie. Premier partie, Terrains triasique et jurassique. Mémoires de l'Académie des Sciences de l'Institut de France 2ème série 54, 1–184.

Fischer, J.-C., 1969. Géologie, paléontologie et paléoécologie du Bathonien en sud-ouest du Massiv Ardennais. Mémoires du Muséum National d'Histoire naturelle de Paris (Série C) 20, 1–319.

Fürsich, F.T., Freytag, S., Röhl, J., Schmid, A., 1995. Palaeoecology of benthic associations in salinity-controlled marginal marine environments: Examples from the Lower Bathonian (Jurassic) of the Causses (southern France). Palaeogeography, Palaeoclimatology, Palaeoecology 113, 135–172.

Goldfuss, G.A., 1837. Petrefacta Germaniae. Theil 2, Lieferung 6. Arnz, Düsseldorf (83 pp.).

Holzapfel, S., 1998. Palökologie benthischer Faunengemeinschaften und Taxonomie der Bivalven im Jura von Südtunesien. Beringeria 22, 3–119.

Jaitly, A.K., Fürsich, F.T., Heinze, M., 1995. Contributions to the Jurassic of Kachchh, western India. IV. The bivalve fauna. Part I. Subclasses Palaeotaxodonta, Pteriomorphia, and Isofilibranchia. Beringeria 16, 147–257.

Lazăr, I., 2006. Jurasicul mediu din Bucegi, versantul vestic. Paleontologie şi paleoecologie. Ars Docendi, Bucaresti, 185 pp.

Lycett, J., 1850. Tabular view of fossil shells from the middle division of the Inferior Oolite in Glouchestershire. The Annals and Magazine of Natural History Second Ser. 6, 401–425.

Lycett, J., 1863. Supplementary monograph on the Mollusca from the Stonefield Slate, Great Oolite, Forest Marble, and Cornbrash. Monograph of the Palaeontographical Society of London 15, 1–129.

Palmer, T.J., 1979. The Hampen Marly and White Limestone formations: Florida-type carbonate lagoons in the Jurassic of central England. Palaeontology 22, 189–228.

Pugaczewska, H., 1986. Bivalvia of the Polish Middle Jurassic and remarks on their palaeoecology. Acta Palaeontologica Polonica 31, 27–83.

Stoll, E., 1934. Die Brachiopoden und Mollusken der pommerschen Doggergeschiebe Abhandlungen aus dem geologisch-palaeontologischen Institut der Ernst Moritz Arndt-Universität Greifswald 13, 1–62.

Todd, J.A., Palmer, T.J., 2002. The Jurassic bivalve genus Placunopsis: new evidence on anatomy and affinities. Palaeontology 45, 487–510.

Yin, J.-R., Fürsich, F.T., 1991. Middle and Upper Jurassic bivalves from the Tanggula Mountains, W-China. Beringeria 4, 127–192.

Table 3. Additional information about stratigraphic range and geographical distribution of gastropods from Oued Craima and Sidi Ouarzik.

GASTROPODA

Species	Stratigraphic range	Geographic distribution	References
***Pseudomelania* (*Oonia*) *variata* (Lycett, 1863)**	Upper Bathonian	north-eastern Paris Basin and south-western England	Lycett (1863); Cossmann (1885); Fischer (1969)
	Undiff. Bathonian	south-western England	Cox and Arkell (1950)
***Eligmoloxus limneiformis* Cossmann, 1885**	Lower Bathonian	north-eastern Paris Basin	Cossmann (1885)
***Exelissa* cf. *binodosa* Gründel, 1990**	Callovian	northern Germany	Gründel (1990, 1999)
***Globularia* cf. *eparcyensis* (d'Archiac, 1843)**	Middle and Upper Bathonian	north-eastern Paris Basin	Fischer (1969); Fischer and Weber (1997)
***Globularia* cf. *tancredi* (Morris & Lycett, 1850)**	(Upper?) Bathonian	south-western England	Cox and Arkell (1950)
***Ampullospira actaea* (d'Orbigny, 1850)**	Middle and Upper Bathonian	north-eastern Paris Basin	Fischer (1953, 1969); Fischer and Weber (1997)
	Undiff. Bathonian	western England	Cox and Arkell (1950)
***Naricopsina matheroni* (Gourret, 1884)**	Undiff. Bathonian	southern France	Cox and Maubeuge (1950)
***Pictavia*? cf. *stricklandi* (Morris & Lycett, 1850)**	Lower to Upper Bathonian	northern Paris Basin	Cossmann (1885)
	Undiff. Bathonian	south-western England	Cox and Arkell (1950)

***Ceritella dewalquei* (Piette, 1857)**	Middle and Upper Bathonian	north-eastern Paris Basin	Fischer (1969)
***Nerinella elegantula* (d'Orbigny, 1850)**	Lower Bathonian to Upper Bathonian	Paris Basin	Fischer (1953, 1969); Fischer and Weber (1997)

References

Cossmann, M., 1885. Contribution a l'étude de la faune de l'étage Bathonien en France (Gastropodes). Mémoires de la Société Géologique de France 3ème série 3, 1–374.

Cox, L.R., Arkell, W.J., 1950. A survey of the Mollusca of the British Great Oolite Series. Primarily a nomenclatorial revision of the monographs by Morris and Lycett (1851–55), Lycett (1863) and Blake (1905–07). Part 2. Monograph of the Palaeontographical Society of London 103, 49–105.

Cox, L.R., Maubeuge, P.-L., 1950. Révision de la faune de mollusques de l'horizon des "Stipites" du Larzac (Bathonien saumâtre). Mémoires de la Société d'études paléontologiques et palethnographiques de Provence 2 (1949), 1–11.

Fischer, J.-C., 1953. Notes sur les gastéropodes d'un niveau gîte coquillier du Bathonien des Ardennes. Journal de Conchyliologie 93, 3–25.

Fischer, J.-C., 1969. Géologie, paléontologie et paléoécologie du Bathonien en sud-ouest du Massiv Ardennais. Mémoires du Muséum National d'Histoire naturelle de Paris (Série C) 20, 1–319.

Fischer, J.-C., Weber, C., 1997. Révision critique de la Paléontologie Française d'Alcide d'Orbigny (incluant la réédition de l'original). Volume II, gastropodes jurassiques. Muséum National d'Histoire Naturelle and Masson, Paris (300 pp.).

Gründel, J., 1990. Gastropoden aus Callov-Geschieben aus dem Norden der DDR. I. Procerithiidae und Mathildidae. Zeischrift für Geologische Wissenschaften 18, 763–773.

Gründel, J., 1999. Procerithiidae (Gastropoda) aus dem Lias und Dogger Deutschlands und Polens. Freiberger Forschungshefte C481, 1–37.

Lycett, J., 1863. Supplementary monograph on the Mollusca from the Stonefield Slate, Great Oolite, Forest Marble, and Cornbrash. Monograph of the Palaeontographical Society of London 15, 1–129.